A.

A METHOD OF PRODUCING A TOWING TANK MODEL OF AN IRREGULAR SEA CONTAINING A CONTINUOUS DISTRIBUTION OF FREQUENCIES

B.

EXPERIMENTAL DETERMINATION OF WAVE FORM AND SHIP RESPONSES MAXIMA IN COMPARISON WITH STATISTICALLY ESTIMATED DATA

by

THEODORE LOUKAKIS

Diploma, National Technical University of Athens
(1962)

SUBMITTED IN PARTIAL FULFILLMENT OF
THE REQUIREMENTS FOR THE DEGREE
OF MASTER OF SCIENCE IN NAVAL
ARCHITECTURE AND MARINE ENGINEERING

at the

MASSACHUSETTS INSTITUTE OF TECHNOLOGY
January 1966

Signature of Author _____
Department of Naval Architecture and
Marine Engineering, January 1966

Certified by _____
Thesis Supervisor

Accepted by _____
Chairman, Department Committee on Graduate Students

ABSTRACT

A. A METHOD OF PRODUCING A TOWING TANK MODEL OF AN IRREGULAR SEA CONTAINING A CONTINUOUS DISTRIBUTION OF FREQUENCIES

B. EXPERIMENTAL DETERMINATION OF WAVE FORM AND SHIP RESPONSES MAXIMA IN COMPARISON WITH STATISTICALLY ESTIMATED DATA

BY

THEODORE LOUKAKIS

Submitted to the Department of Naval Architecture and Marine Engineering on January 1966 in partial fulfillment of the requirements for the degree of Master of Science in Naval Architecture and Marine Engineering

A. Wave tapes modeling irregular seas were produced by feeding white noise into a filter whose frequency response has been determined from the Pierson-Moskowitz spectral form, and recording the output.

The tapes were tested and the spectral density of the wave forms made by the tapes was found to be a very close approximation to the Pierson-Moskowitz spectral form.

B. The model of a fast cargo ship was tested in different sea states. Long data was accumulated from the results of several runs. The apparent heights of the wave form, the pitching and heaving motions, and the longitudinal wave bending moment were examined for their statistical distribution. The values of $\tilde{H}^{(P)}/\tilde{H}_{R.M.S.}$ were found to follow approximately the Rayleigh probability density distribution for values of $1/m$ up to 1/50 and then depart and level off as an expected natural cut-off occurs.

ACKNOWLEDGEMENTS

The author wishes to express his gratitude to his supervisor, Professsor Martin A. Abkowitz, for his continuous advice and guidance. The precious help of Professor Justin E. Kerwin is also much appreciated.

Thanks are also due to Mr. Frank Sellars for his guidance and assistance.

All machine computations were executed by the IBM Digital Computer at the Computation Center of Massachusetts Institute of Technology.

TABLE OF CONTENTS

LIST OF SYMBOLS

$\tilde{A}_c$	Apparent crest amplitude
$\tilde{A}_T$	Apparent trough amplitude
$\bar{f}$	Dimensionless frequency
$H(\omega)$	Complex frequency response of a system Transfer function of a system
$H(\theta)$	Error function
$\tilde{H}$	Apparent height
$\tilde{H}^{(p)}$	The 1/n -p highest apparent heights of a random process
$\tilde{H}_{R.M.S}$	The root mean square apparent height
$h(\alpha)$	The impulse response function
m_n	The nth moment of the spectral density function
$P_f(\eta)$	Probability density function of a random variable
$Q_f(\eta)$	Cumulative probability distribution function of a random variable
r	Proportion of negative maxima
$\delta(\alpha)$	Dirac delta function
ε	Broadness factor
ζ	Damping ratio
η	Experimental value of a random variable. Normalized maximum of a random variable.
$\eta^{(1/n)}$	The 1/n highest values of a random variable
$\equiv$	Departure of a stationary point of a random process from the zero mean line
ξ	Experimental value of
σ^2	Variance of a random function
τ	Time shift

$\hat{\Phi}(\omega)$	One-sided spectral density function
$\hat{\Phi}_o$	White noise spectral density function
Φ	Dimensionless spectral density function
$\varphi(\alpha)$	One dimensional autocorrelation function
ω	Circular frequency
ω_r	Circular frequency of the maximum spectral density
ω_n	Natural circular frequency of a filter

LIST OF FIGURES

PART A

A METHOD OF PRODUCING TOWING TANK MODEL OF IRREGULAR SEAS CONTAINING A CONTINUOUS DISTRIBUTION OF FREQUENCIES

1. INTRODUCTION

Seakeeping tests in a ship model towing tank require an exact representation of the actual sea.

The major problem for a model of a sea state is to have an accurate representation of the elevation of the water surface in both its statistical distribution and energy spectrum.

For the elevation of the sea surface above the calm water level there is general agreement among the oceanographers that it is distributed according to the Gaussian probability density distribution.

For the wave energy spectra, the surface oceanography has not produced up to now enough data to reliably define a typical, at least for a region of the oceans, wave energy spectrum. Therefore one has to choose among the different formulations to find the one he feels conforms better with reality.

The current practice in the Department of Naval Architecture and Marine Engineering of Massachusetts Institute of Technology is to use the spectral form for fully developed wind seas proposed by W. J. Pierson and L. Moskowitz [1]* and based on the similarity theory of S. A. Kitaigorodskii.

The method of producing waves at the model towing tank which conforms with the above two requirements is described below. Although the Pierson-Moscowitz spectrum was used for the production of the tapes, it is very easy to produce wave tapes with any desirable wave energy spectrum which possess the Gaussian probability density distribution.

---

* Numbers in square brackets denote references.

2. DESCRIPTION OF THE METHOD

2.1 White Noise

The basic concept in the method is the one of the white noise [2]. By definition, ideal white noise is a process that has uniform spectral density for all frequencies Fig. (1) .

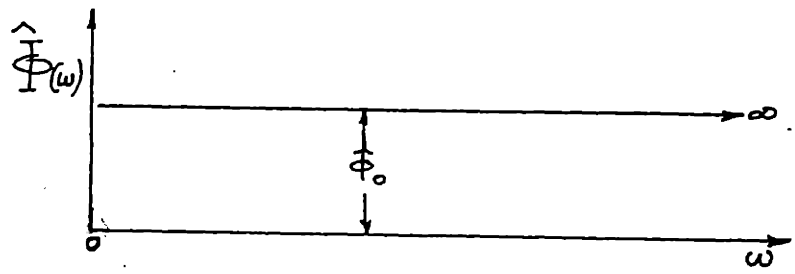

Fig. 1 White Noise Spectrum

A mathematical model of white noise is a Poisson wave of equally likely positive and negative unit impulses [3] .

The concept of ideal white noise is a physically unrealizable one since the mean square value of such a process would be infinite because of the infinite area under the spectrum. Nevertheless the band-limited white noise Fig. (2) is a model that is a close approximation to many physically realizable random processes. For example, an electromagnetic random shaker can be adjusted to provide acceleration processes with white noise type spectra and a gas tube is a source of white noise.

The time history of a sample function of white noise can be seen in Fig. (12).

For our analysis a band-limited nominally white noise was supplied

by a noise source generator* that was assumed to have a uniform spectral density over the range 0-20 KC.

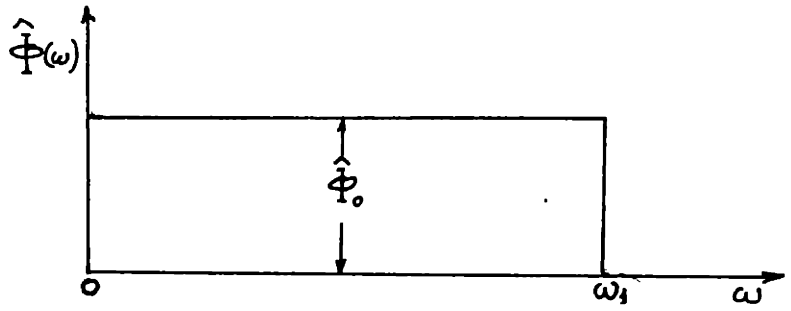

Fig. 2 Spectral Density of Band Limited White Noise

* Noise Source Model UPN by Philbrick Researches, Boston, Massachusetts

2.2 Response to White Noise

Let's have an excitation $x(t)$ and a linear time invariant system Fig. (3) . The response of the system to the excitation $x(t)$ is given by the superposition or convolution integral:

$$y(t) = \int_0^\infty x(t-\tau)\, h(\tau)\, d\tau \qquad (2.1)$$

where $h(\tau)$ is the impulse-response function; that is, the response of the system to the excitation $\delta(\tau)$, the Dirac-delta function.

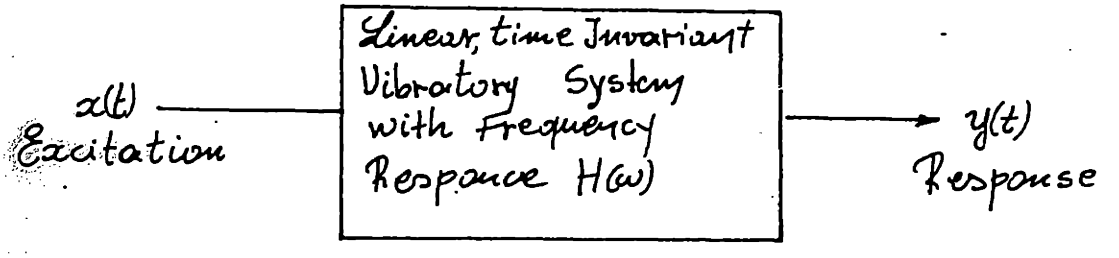

Fig. 3

The complex frequency response $H(\omega)$ of the system (transfer function of the system) is defined as the Fourrier transform of $h(t)$ or

$$H(\omega) = \int_0^\infty h(t) e^{-i\omega t}\, dt \qquad (2.2)$$

The above relations hold for the input-output relation for linear time invariant systems in terms of particular responses to particular excitations.

When the excitation is a random process we know that:

a. When the excitation is an ergodic random process then the response is also an ergodic random process and eq. 2.1 holds for any individual sample excitation and response

b. For ergodic random processes, the input-output relation for spectral densities is:

$$\hat{\Phi}_{y(\omega)} = |H(\omega)|^2 \hat{\Phi}_{x(\omega)} \qquad (2.3)$$

where $H(\omega)$ is the complex frequency response (or transfer function) of the system. We note that only the magnitude of the transfer function is needed and therefore we do not have to know the phase relation of the input and output.

When the input is white noise with constant spectral density over the range of frequencies we are interested in, eq.2.3 becomes:

$$\hat{\Phi}_{y(\omega)} = |H(\omega)|^2 \hat{\Phi}_0 \qquad (2.4)$$

For the white noise we know that it is an ergodic process and therefore the output is going to be an ergodic process, too. Furthermore, we know that the white noise is a normal or Gaussian* process and this means that the output is going to be a normal process.

The above two properties that the output is going to possess are in accordance with the assumptions and measurements made for sea elevations in both theoretical and experimental work.

Note: In reality the statistical distribution of the white noise produced by the generator used is the sum of two Rayleigh distributions such that their sum is a close approximation of normal distribution.

3. The Frequency Response of the Filter

The idea of the method used is to build a filter with such a transfer function that when excited by white noise the spectral density of the output is the one given by the Pierson-Moskowitz spectral form. The spectral density of the Pierson-Moskowitz spectrum is given by the relation:

$$\hat{\Phi}(\omega) = \frac{8.1\times10^{-3} g^2}{\omega^5} e^{\left[-0.74\left(\frac{g}{V\omega}\right)^4\right]} \qquad (3.1)$$

where: $\hat{\Phi}(\omega)$ = the spectral density

ω = the circular frequency

g = the acceleration of gravity

V = the wind velocity

This relation is valid for any set of consistent units. In Fig. (4) appear several energy spectra with spectral density given by (3.1). From relations (2.4) and (3.1) we see that we can determine the required transfer function of the filter (to be exact, the modulus of the transfer function) as:

$$|H(\omega)| = \left(\frac{\hat{\Phi}_y(\omega)}{\hat{\Phi}_0}\right)^{1/2} \qquad (3.2)$$

Since $\hat{\Phi}_0$ = constant the above relation suffices to determine the modulus of transfer function of the filter (within a constant).

At first sight, it appears that we have to build one filter for every wind speed. This is not the case as the Pierson-Moskowitz spectrum can be plotted in non-dimensional form as in Fig.(5) where:

$\bar{f} = \frac{Vf}{g}$ = the dimensionless frequency (3.3)

and $\bar{\Phi}(\bar{f}) = \frac{\hat{\Phi}(f) g^3}{V^5}$ = the dimensionless spectral density (3.4)

$f = \frac{\omega}{2\pi}$ = the frequency

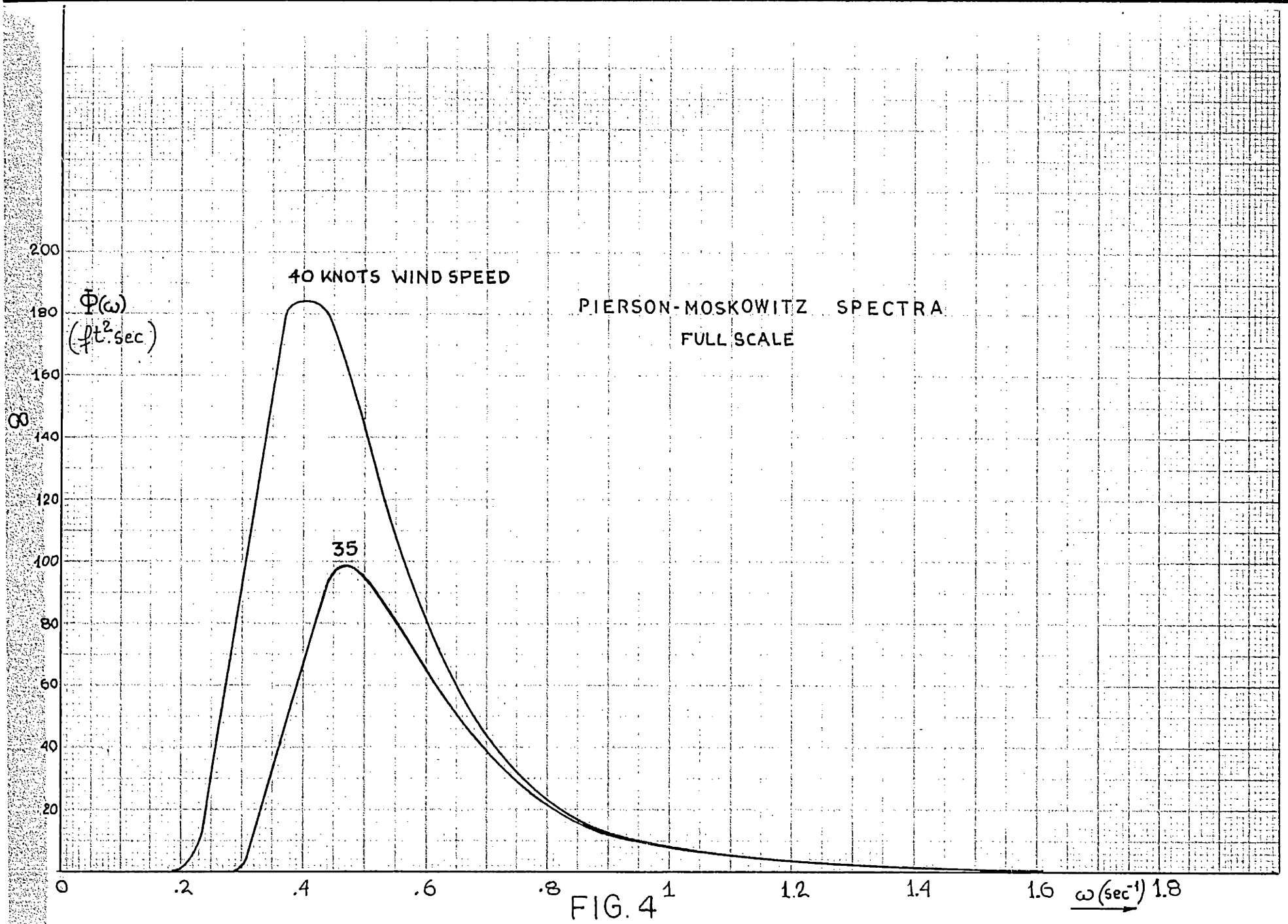
PIERSON-MOSKOWITZ SPECTRA
FULL SCALE
40 KNOTS WIND SPEED
35
Φ(ω)
(ft².sec)
ω
200
180
160
140
120
100
80
60
40
20
0
.2
.4
.6
.8
1
1.2
1.4
1.6
ω (sec⁻¹)
1.8

FIG. 4

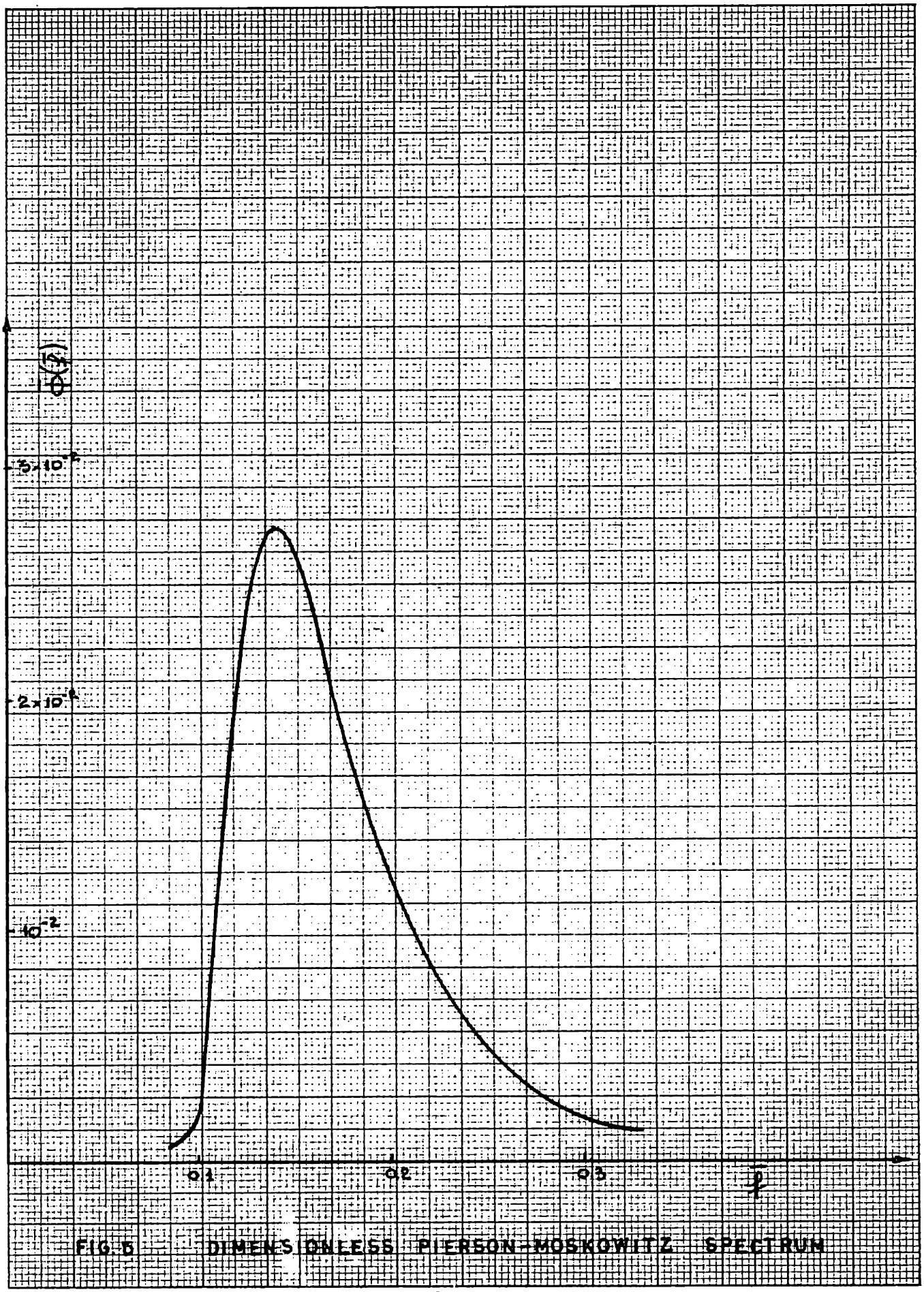

FIG. 5 DIMENSIONLESS PIERSON-MOSKOWITZ SPECTRUM

Therefore we see that by shifting the frequency of the max response and changing the magnitude of $\hat{\Phi}_o$ we can have as output any spectrum of the family for which the filter is designed.

The above is true when the construction of the filter permits the versatility of shifting the frequencies. This is the case when the filter is "built" in the analog computer with operational amplifiers.

When the filter is constructed from components, it is valid only for one particular spectrum, unless the possibility of changing components is provided (For a computerized method of determining the necessary components of a filter when we know the modulus of the frequency response see [4]).

By comparing the two methods of constructing the filter, we can say that the second one gives more accurate results and it is probably the only practical approach when we are dealing with spectra of different form than the one in Fig. (4), e.g. the spectrum of fully developed seas containing a swell. But each filter is valid only for one wind speed and the actual construction is much more time consuming and expensive than the second one.

The analog computer solution is much simpler, is less expensive and one can, in a single day, produce several tapes of various wind speeds. The accuracy of the method is quite satisfactory if we have in mind that the analytical expression for the spectral density is nothing else than curve fitting of experimental data and even the frequency of the maximum response is subjected to further experimentation.

4. Construction of the Filter in the Analog Computer

A filter with a transfer function very close to the ideal was achieved by cascading several second order systems.

In fact three high pass and one low pass filters were used.

The required transfer function* is found by converting the particular wave spectrum in model scale and taking the square root of the ordinates Fig. (6) according to 3.2. By erecting a vertical at the frequency of the maximum ordinate ω_r we divide the spectrum into two parts. (We can find exactly ω_r from 3.3 by setting:

$$\bar{f} = 0.1336 \quad (4.1).)$$

The rigth part, including the tail of the spectrum, is going to be given by the low pass filter.

The natural frequency of the low pass filter is going to be approximately ω_r. The other characteristic of the filter that is needed is ζ, the damping ratio of the filter. We select a filter** that has the same ratio $\frac{\omega_{P.P.}}{\omega_n}$ as our required transfer function, where $\omega_{P.P.}$ Fig. (6) is the frequency of the half-power point of the right part of the spectrum defined by the the relation

$$\frac{|H(\omega)|_{P.P}}{|H(\omega)|_{max}} = \frac{1}{\sqrt{2}} \qquad (4.2)$$

The left part of the filter is going to be given by a cascade of high pass filters and this is a trial and error process.

For a cascade of four filters Fig. (7)

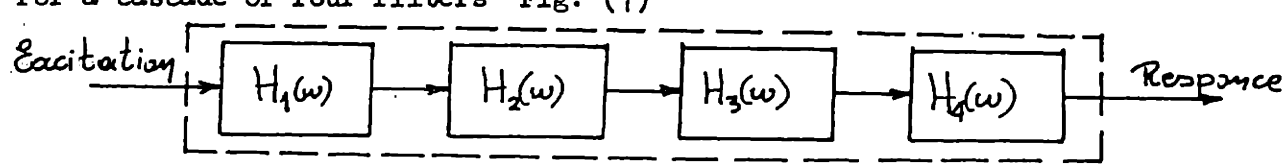

Figure 7

* All the numerical values of the paragraph apply to 40 knots wind wave spectrum.
** In Ref. (5) there is a logarithmic plot of $|Hw|$ for several values of ζ.

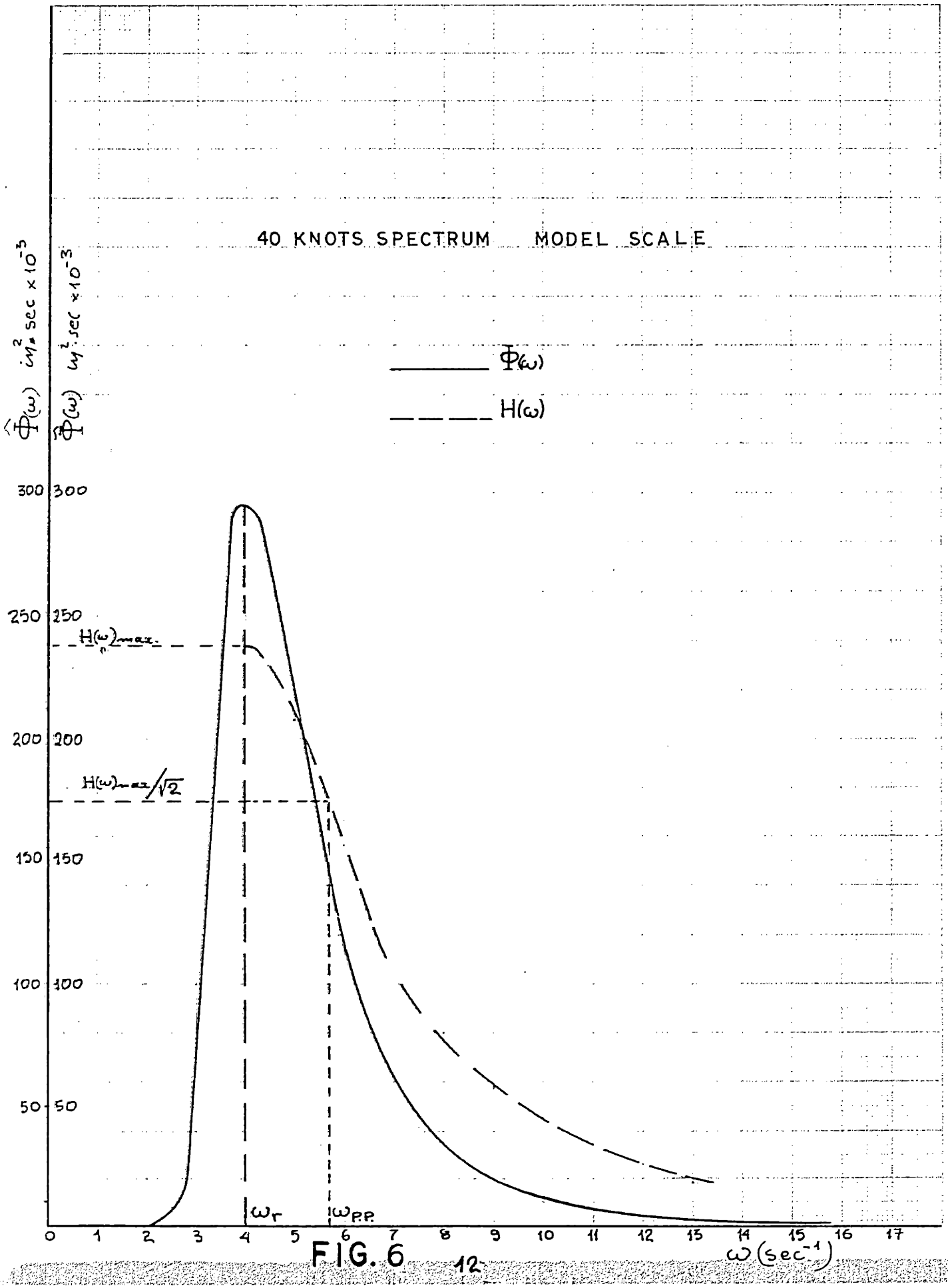
40 KNOTS SPECTRUM MODEL SCALE
Φ(ω)
H(ω)
Φ(ω) in² sec x 10⁻³
Φ(ω) ft² sec x 10⁻³
300
250
200
150
100
50
H(ω)max
H(ω)max/√2
ωr
ωP.P.
0 1 2 3 4 5 6 7 8 9 10 11 12 13 14 15 16 17
ω (sec⁻¹)

FIG. 6

the transfer function of the system is given by:

$$|H(\omega)| = |H_1(\omega).H_2(\omega).H_3(\omega).H_4(\omega)| \quad (4.3)$$

We are using one low pass filter and three identical high pass filters. By taking the logarithm of both parts of eq. (4.3) we get:

$$\log|H(\omega)| = \log|H(\omega)_{lowpass}| + 3\log|H(\omega)_{highpass}| \quad (4.4)$$

We normalize the desired transfer function to have a maximum value equal to the maximum value of the transfer function of the low pass filter which is given by:

$$|H(\omega)_{lowpass}| = \frac{1}{\left\{\left[1-\left(\frac{\omega}{\omega_n}\right)^2\right]^2 + \left[\frac{2\zeta\omega}{\omega_n}\right]^2\right\}^{1/2}} \quad (4.5)$$

and we transform all the other ordinates by the same ratio.

We plot the transfer function of the low pass filter in logarithmic paper and we measure the ratio $\frac{\omega_{max.ordinate}}{\omega_n}$.

Since we want to have peak response at ω_r we put $\omega_{max.ord.} = \omega_r$ and we plot the transfer function accordingly.

The left part of the transfer function can be approximated by the cascade of the high pass filters. The choice of natural frequency and damping ratio of the high pass filters is achieved by trial and error. The natural frequency that corresponds to $\omega/\omega_n = 1$ of the plot is the one of the low pass filter and the transfer function of each of the high pass filters is given by:

$$|H(\omega)_{highpass}| = \frac{\left(\omega/\omega_n\right)^2}{\left\{\left[1-\left(\frac{\omega}{\omega_n}\right)^2\right]^2 + \left[\frac{2\zeta\omega}{\omega_n}\right]^2\right\}^{1/2}} \quad (4.6)$$

where ω_n and ζ are the ones corresponding to the high pass filter.

From Fig. (8) we see that the approximate transfer function is very close to the desired one.

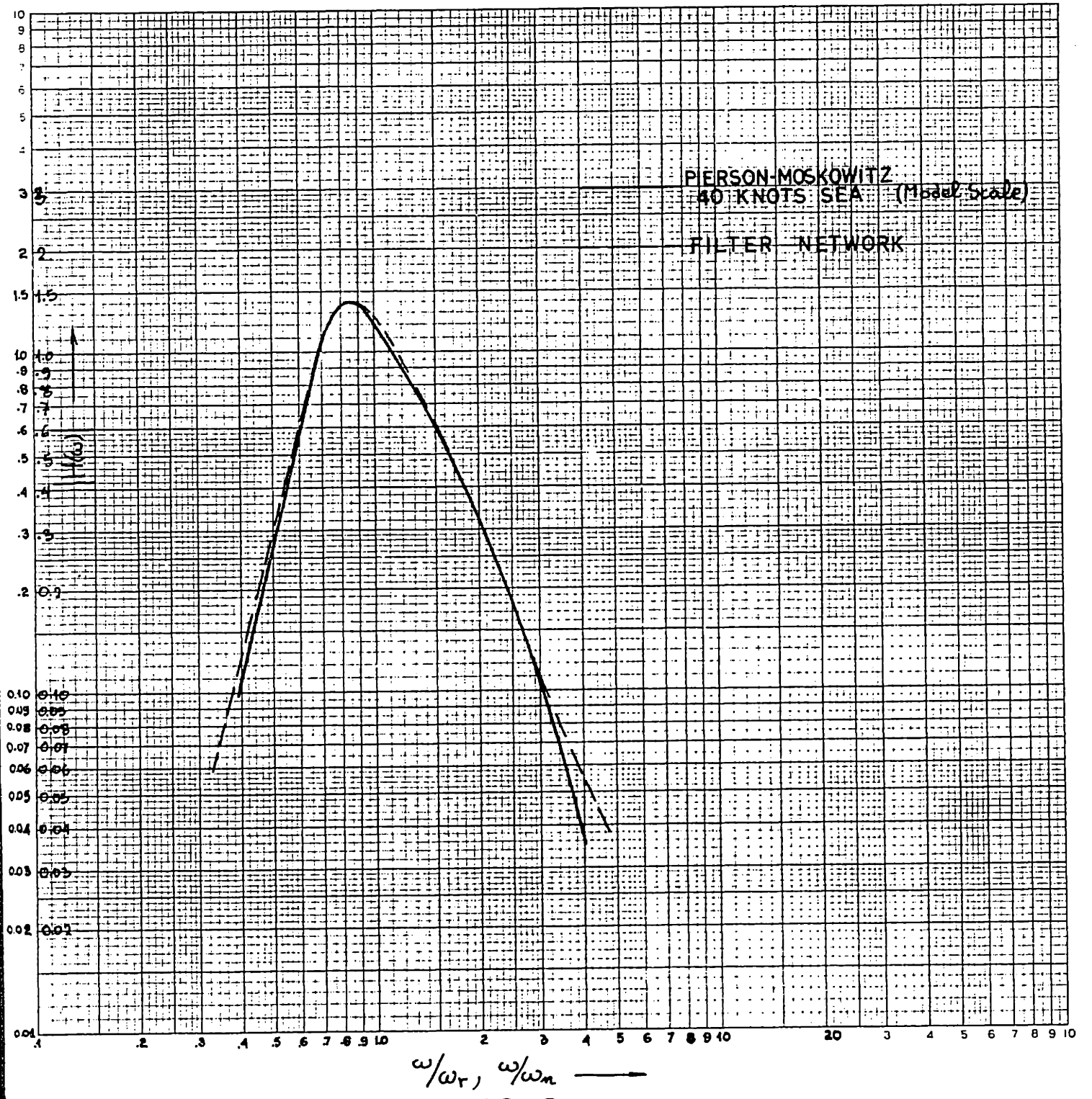

FIG. 8

ull Logarithmic, 3 × 3 Cycles

The fact that the slope of the tail is smaller than the slope of the desired transfer function is not important because this divergence occurs at $\omega/\omega_r \approx 4$ and from the wave spectrum we find that the spectral density at this range is negligible compared with the maximum value (0.3% .)

After the characteristics of the filters have been determined we simulate the cascade of filter in the analog computer.

Three K5-U Universal Linear Operators made by Philbrick Researches, Boston, Massachusetts were used for each filter.

The analog computer diagram of the cascade appears in Fig. (9).

The transfer function of the filter was tested by means of an oscillator with sine waves at several points. The analog computer diagram of the oscillator appears in Fig. (10). Two K5-U operational amplifiers are needed for the oscillator.

The desired transfer function is plotted in Fig. (11) against the results of the oscillator test.

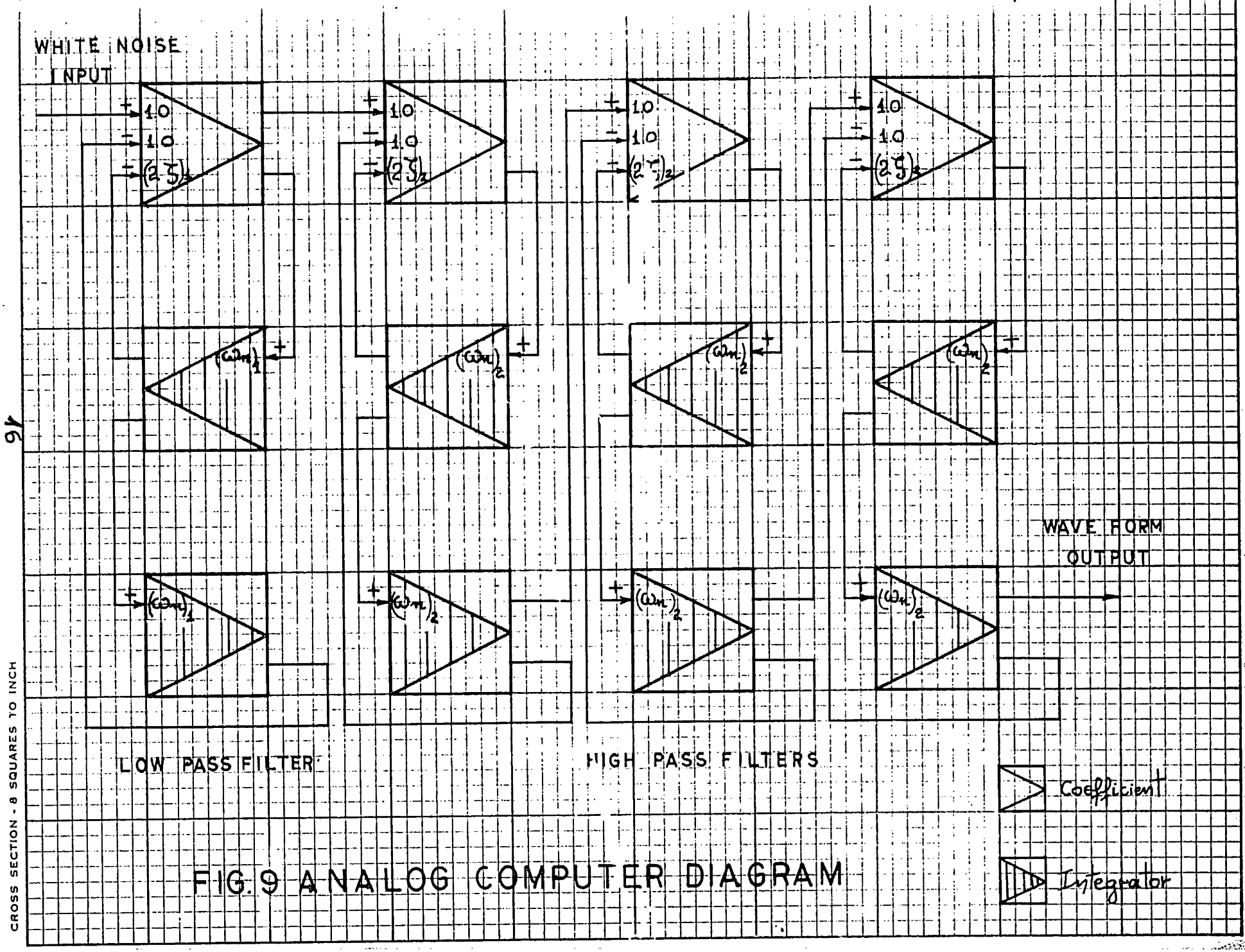

FIG. 9 ANALOG COMPUTER DIAGRAM

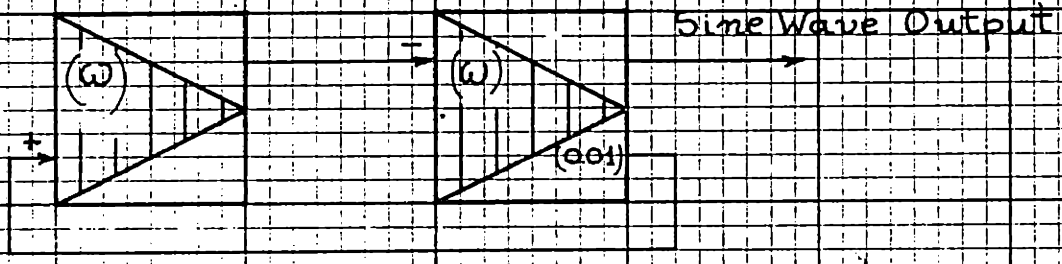

FIG. 10 ANALOG COMPUTER DIAGRAM OF OSCILLATOR

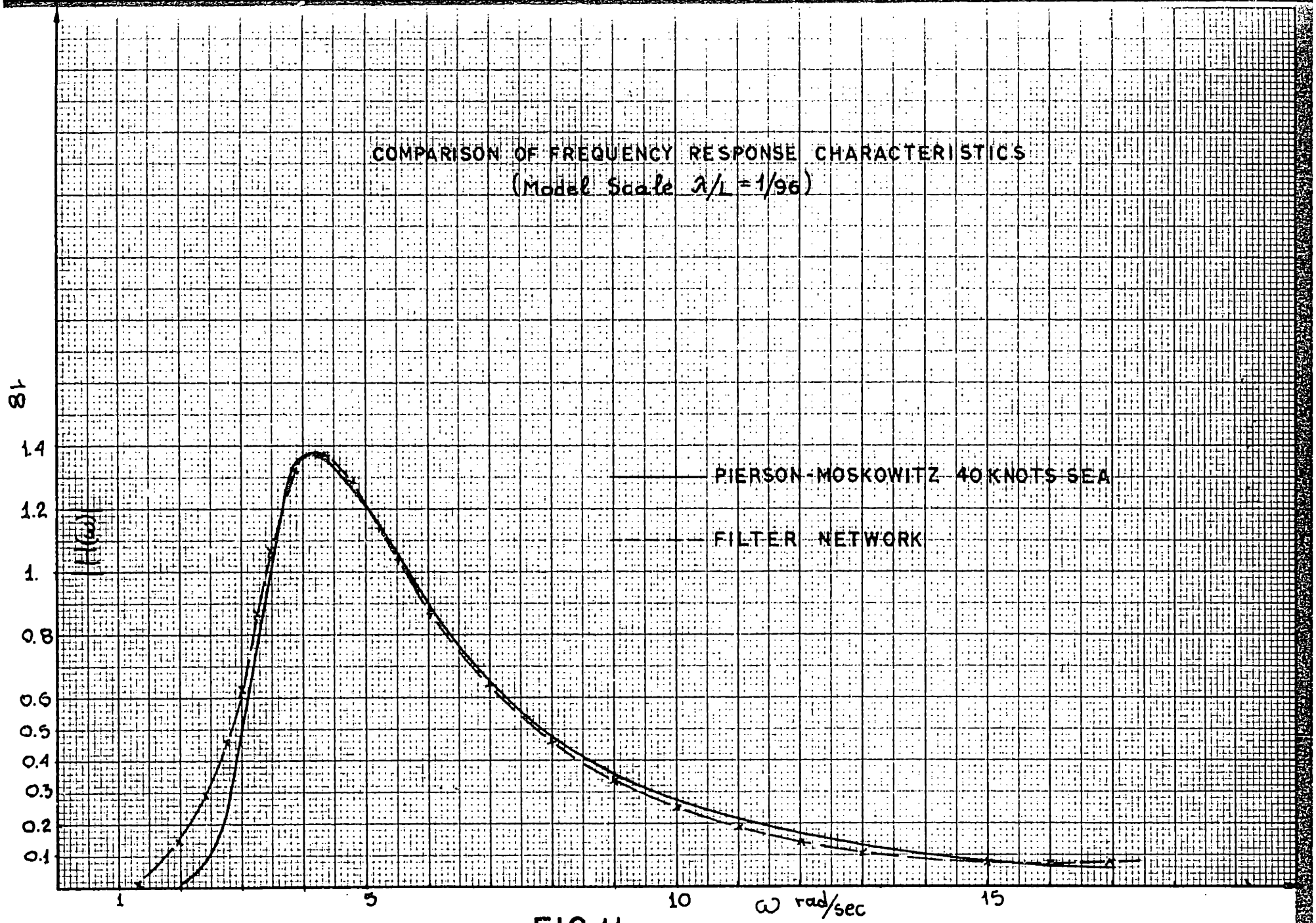
COMPARISON OF FREQUENCY RESPONSE CHARACTERISTICS
(Model Scale λ/L = 1/96)
PIERSON-MOSKOWITZ 40 KNOTS SEA
FILTER NETWORK
18
1.4
1.2
1.
0.8
0.6
0.5
0.4
0.3
0.2
0.1
1
5
10
15
ω rad/sec

FIG.11

5. Calibration of the Output

The output of the white noise generator is fed into the cascade of filters and the output of the filters is the desired wave form. A long sample of the wave form, adequate for seakeeping experiments, is recorded on tape.

In Fig. (12) appear both the white noise input and the wave form output.

The white noise is spectroanalyzed by a combination of dynamic analyzer and sweep oscillator* and the value of his spectral density $\hat{\Phi}_o$ is found.

The tape with the wave form is used to excite the servo-controlled hydraulic valve of the towing tank paddle-type wavemaker. The transfer function of the hydraulic valve-paddle system is a constant.

Hence, since we know the spectral density of the white noise, the transfer function of the filter and the fact that the transfer function of the hydraulic valve- paddle system is a constant, we can calibrate the record, by a sine wave recorded on it, so that we get the spectral density we need for the actual waves that are produced in the tank.

---

* Dynamic Analyzer SD -1017
Sweep Oscillator SD104-5 } by Spectral Dynamics Corporation, San Diego, California

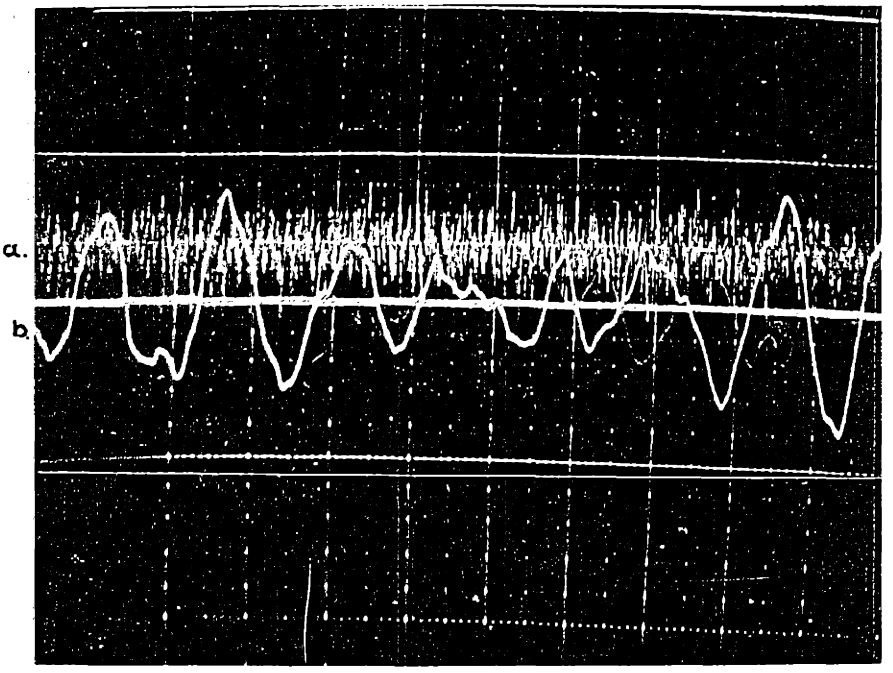

Figure 12

a. White Noise Input

b. Wave Form Output

6. Discussion of the Results

The tapes made by the new method were tested in the towing tank at Massachusetts Institute of Technology.

The waves produced by these tapes were recorded on tape and then digitized at M.I.T.'s Computation Center. The digital data was spectro-analyzed and the results appear in Figs. (13) and (14).

The results are in close agreement with the Pierson-Moskowitz spectra. The slight shift of the peak frequency is in accordance with the frequency response characteristics of the filter network Fig. (11) and is caused by the high pass filters.

Overall, the results are quite satisfactory for seakeeping tests with random seas.

Spectral analysis was done with 60 and 180 lags with satisfactorily comparable results. Also, the command signal was spectroanalyzed and the spectrum was found to be practically the same with the wave spectrum thus proving that the hydraulic valve-paddle system has a constant transfer function.

As a final note we can add the comparison of the wave form recorded in the towing tank to actual wave records from [6], where we note the apparent similarity of the two records Fig. (15) .

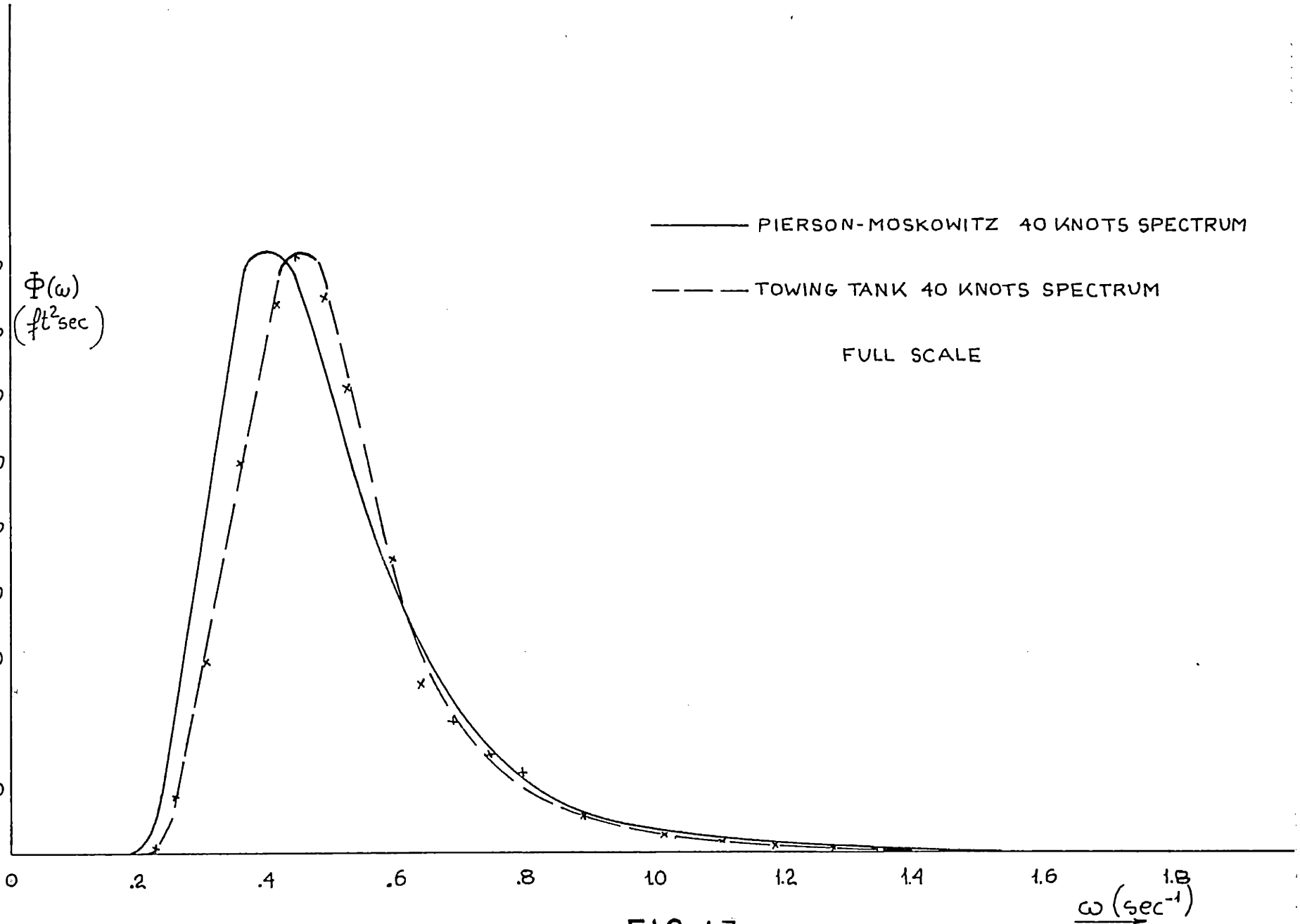
PIERSON-MOSKOWITZ 40 KNOTS SPECTRUM
TOWING TANK 40 KNOTS SPECTRUM
FULL SCALE
Φ(ω)
(ft² sec)
180
160
140
120
100
80
60
40
20
0
.2
.4
.6
.8
1.0
1.2
1.4
1.6
1.8
ω (sec⁻¹)

FIG. 13

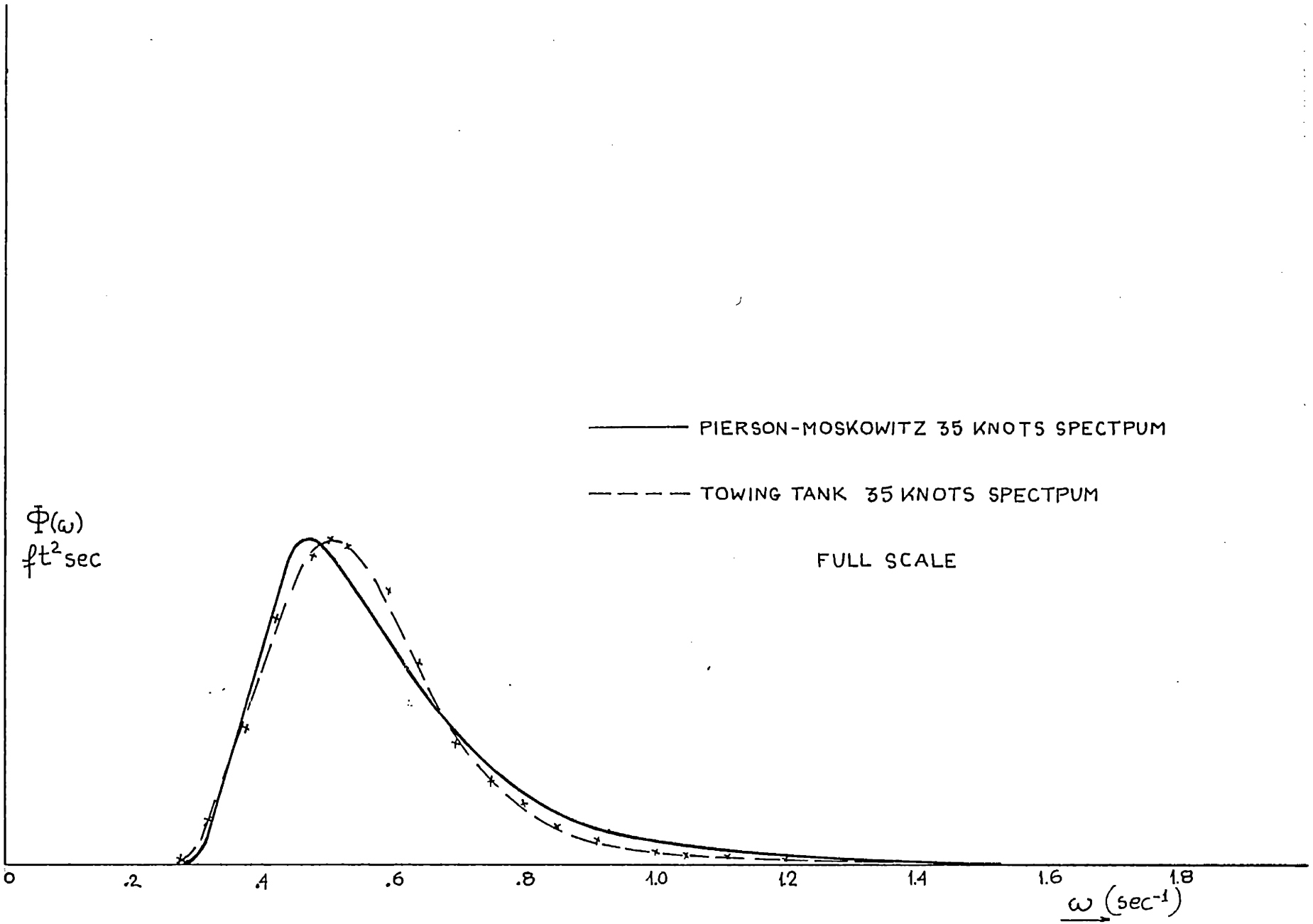
PIERSON-MOSKOWITZ 35 KNOTS SPECTPUM
TOWING TANK 35 KNOTS SPECTPUM
FULL SCALE
Φ(ω)
ft² sec
120
100
80
60
40
20
0
.2
.4
.6
.8
1.0
1.2
1.4
1.6
1.8
ω (sec⁻¹)

FIG.14

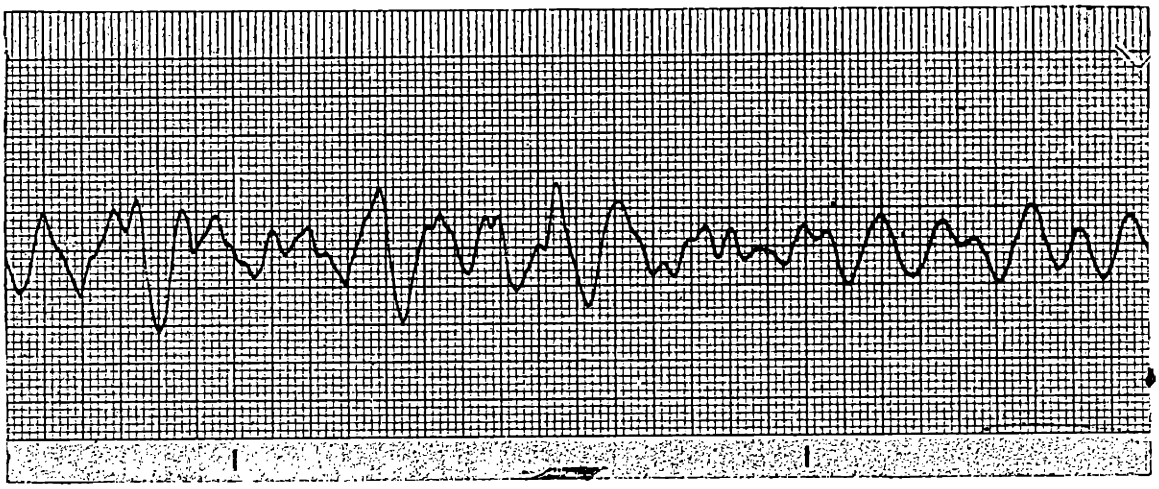

a) Towing Tank Record

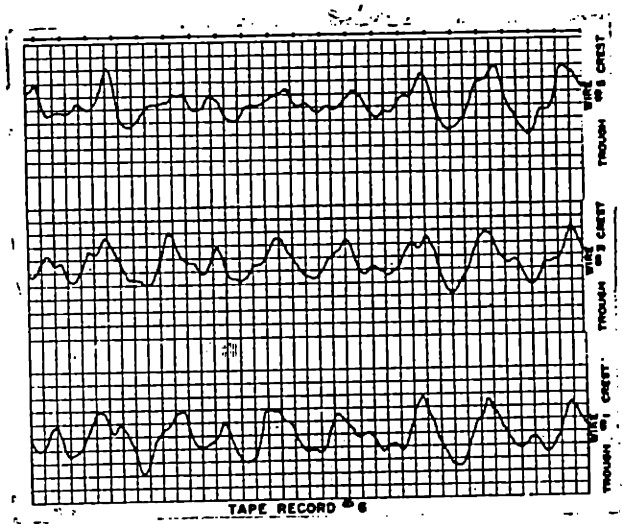

b) Actual Wave Record

Figure 15

LIST OF REFERENCES

PART A

1. Pierson, W. J. and Moskowitz, L., "A Proposed Spectral Form for Fully Developed Wind Seas Based on the Similarity Theory of S. A. Kitaigorodsii," N. Y. University, Geophysical Sciences Laboratory Report 63-12, 1963.
2. Crandall, S. H. and Mark W. D., "Random Vibration in Mechanical Systems," Academic Press, New York, 1963.
3. Lee, Y. W., "Statistical Theory of Communication," Wiley, 1960.
4. Milgram, J. H., "Compliant Water Wave Absorbers," M.I.T., Department of Naval Architecture and Marine Engineering, Report No. 65-13.
5. Shearer, J. L., Murphey, A. T., Richardson, H. H., "Dynamic Systems," Vol. II, Addison-Wesley, 1965.
6. Kinsman, B., "Wind Waves," Prentice-Hall, 1965.

PART B

EXPERIMENTAL DETERMINATION OF WAVE FORM AND SHIP RESPONSES MAXIMA IN COMPARISON WITH STATISTICALLY ESTIMATED DATA

1. INTRODUCTION

1.1 Scope of the Thesis

The maxima of the wave system and the ship responses are random phenomena not following any law from first sight. But in recent years the fields of Oceanography and Seakeeping have experienced considerable progress and several investigators have both theoretically postulated and experimentally proved that the seaway and the ship responses (including their maxima) do follow probabilistic laws in all aspects.

The scope of the sequel is to compare the experimental results of the statistical distribution of the maxima of the wave system and some ship responses (namely: pitch, heave and longitudinal wave bending moment) to results obtained by theoretical tools.

One of the expected results is the determination of the threshold where nature stops following the formally derived statistical expressions and to connect the information so obtained with practical aspects of the maxima of the wave system of the ship responses.

1.2 Definitions

In this paragraph we are going to clarify all the notions and terms used in what follows.

a) The one-dimensional autocorrelation function $\varphi(\tau)$ of a continuous random function of time $f(t)$ is defined as:

$$\varphi(\tau) = \lim_{T\to\infty} \int_0^T f(t) f(t+\tau)\, dt \qquad (1.1)$$

where τ is the time shift and $0 \leq \tau \leq \infty$

b) The spectral density function $\hat{\Phi}(\omega)$ of $f(t)$ is defined as:

$$\hat{\Phi}(\omega) = \frac{1}{2\pi} \int_0^\infty \varphi(\tau) \cos(\omega\tau)\, d\tau \qquad (1.2)$$

i.e. the Fourrier transform of the autocorrelation function.

From (1.1) and (1.2) follows that:

$$\varphi(0) = \overline{f(t)^2}^t = \lim_{T\to\infty} \int_0^T f(t)^2\, dt = \int_0^\infty \hat{\Phi}(\omega)\, d\omega \qquad (1.3)$$

and if $f(t)$ is assumed to be a zero mean process we get:

$$m_0 = \sigma^2 = \overline{f(t)^2}^t = \int_0^\infty \hat{\Phi}(\omega)\, d\omega \qquad (1.4)$$

where σ^2 is the variance of $f(t)$ and m_0 is defined as:

c) The zero moment of $\hat{\Phi}(\omega)$ about the origin, or more generally, we write:

$$m_n = \int_0^\infty \hat{\Phi}(\omega)\, \omega^n\, d\omega \qquad (1.5)$$

for the nth moment of $\hat{\Phi}(\omega)$ about the origin.

d) Specification of a random time series $f(t)$.

In the following self-explanatory figure appears the terminology used in connection with $f(t)$.

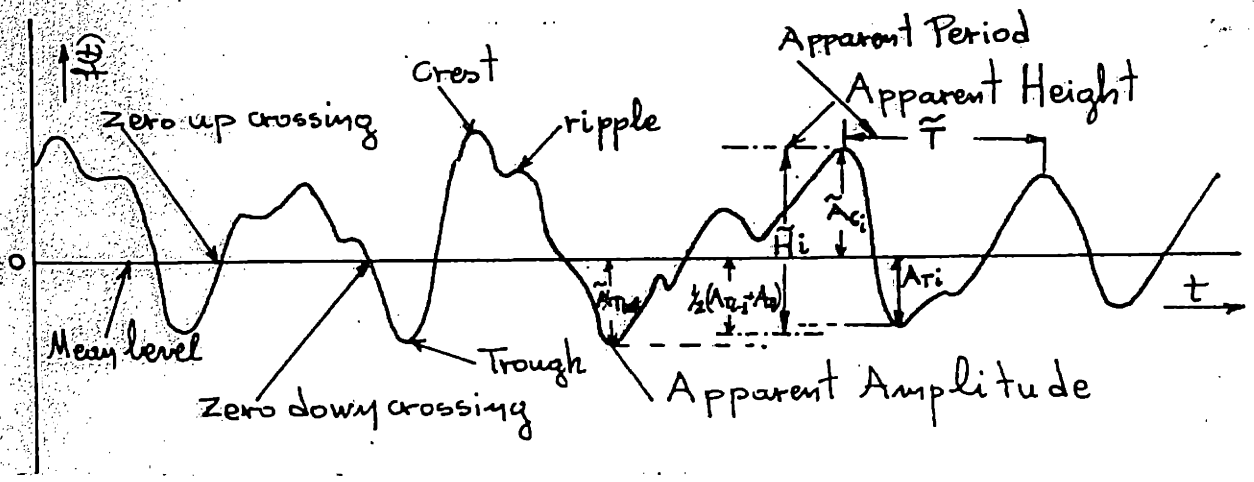

Figure (1)
Specification of a random time series

According to Fig. (1) the apparent height $\tilde{H}$ is defined as the sum of a crest and the average of the preceding and following troughs. The reason for this novel definition (In the literature $\tilde{H}$ is defined, usually, as the sum of a crest and a trough) is explained in the sequel.

e) Narrow and wide ban processes

A random process is considered to be of the narrow band type when the area under its spectral density function is concentrated in the vicinity of a dominant frequency and its spectral density possesses only one peak.

The time history of a narrow band process is of the nature of a sinusoid with slowly varying amplitude.

A random process is considered to be of the wide band type either if its spectral density function possesses more than one peak or if the area under its spectral density is distributed over a relatively broad range of frequencies.

As a characteristic of its time history we can say that it possesses a large number of ripples.

The rigorous distinction between a narrow and a wide band process

is not very well defined. The only analytical tools in our hands are the broadness factor ε,[3], defined as:

$$\varepsilon = 1 - \frac{m_2^2}{m_0 m_4} \tag{1.6}$$

and the proportion of negative maxima r,[3], defined as:

$$r = \frac{1}{2}\left(1 - \frac{N_0^+}{N_1}\right) \tag{1.7}$$

where: N_0 the average density of zero up crossings and N the total density of maxima.

The broadness factor and r are connected by the relation:

$$r = \frac{1}{2}\left[1 - (1-\varepsilon^2)^{1/2}\right] \tag{1.8}$$

When ε assumes the limiting value of 0 the process is characterized as an ideal narrow band process and when assumes the limiting value of 1 the process is characterized as an ideal wide band process.

f) Rayleigh probability density distribution

The probability density function of a random variable f which is Rayleigh distributed is given by: [8]

$$P_f(\eta) = \begin{cases} \frac{2}{K} e^{-\frac{\eta^2}{K}} & \text{for } \eta \geq 0 \\ 0 & \text{for } \eta < 0 \end{cases} \tag{1.9}$$

The mean of f is given by:

$$\bar{f} = \left(\sqrt{\pi}/2\right) K^{1/2} \tag{1.10}$$

The variance of f is given by:

$$\sigma_f^2 = \left(1 - \pi/4\right) K \tag{1.11}$$

From (1.9) and (1.10) it follows that K is the mean squared value of f.

The cumulative probability distribution function of f is given by:

$$Q_f(\eta) = 1 - e^{-\frac{\eta^2}{K}} \tag{1.12}$$

where $$Q_f(\eta) = \int_0^{\eta} P_f(\eta)\, d\eta \tag{1.13}$$

denotes the probability that $f \leq \eta$

2. THE STATISTICAL DISTRIBUTION OF THE MAXIMA OF A RANDOM FUNCTION

2.1 The probability density function of the envelope of an ideally narrow band process

A random process f(t) can be said to represent a narrow band process if f(t) is represented in the form [1] :

$$f(t) = F_c(t)\cos\omega t + F_s(t)\sin\omega t \qquad (2.1)$$

in which ω is a known frequency, whereas $F_c(t)$ and $F_s(t)$ are independent normally distributed random variables with mean=0 and equal variances σ^2 .

From the above definition we see that f(t) is also normally distributed with zero mean and variance .

The envelope of f(t) is then defined as:

$$E(t) = \left[F_c^2(t) + F_s^2(t)\right]^{1/2} \qquad (2.2)$$

According to a result of the probability laws of a function of random variables [2] , if Fc(t) and Fs(t) are independent random variables each normally distributed with mean = o and variance σ^2, then the probability density function of $\left[F_c^2(t)+F_s^2(t)\right]^{1/2}$ is given by:

$$P_{\left[F_c^2(t)+F_s^2(t)\right]}(\eta) = \frac{\eta}{\sigma^2}\, e^{-\frac{1}{2}\left(\frac{\eta}{\sigma}\right)^2} \qquad (2.3)$$

and therefore is Rayleigh distributed. In the light of the above and eq. (1.9) it turns out that the envelope, Fig. (2) , of f(t) is Rayleigh distributed and its mean squared value is given by:

$$\overline{E(t)^2}^t = 2\sigma^2 = 2\,\overline{f(t)^2}^t \qquad (2.4)$$

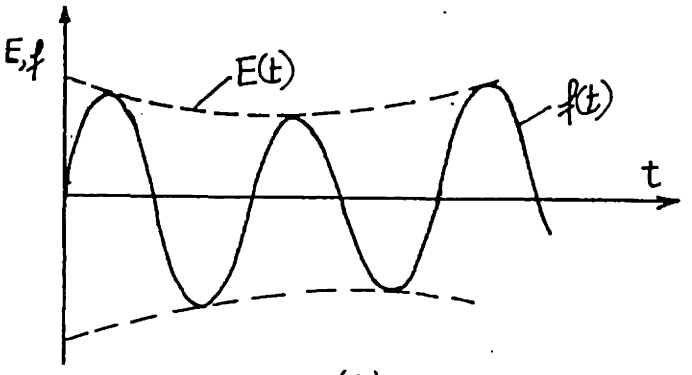

Figure (2)
Narrow Band Process and Envelope

For an alternative derivation of the same result see [5] .

2.2 Calculation of the 1/n highest values of a Rayleigh distributed random variable E(t)

Let E(t) have a Rayleigh probability density distribution given by:

$$P_E(\eta) = \frac{2\eta}{\overline{\eta^2}}\, e^{-\frac{\eta^2}{\overline{\eta^2}}} \qquad 0 \le \eta \le \infty \tag{2.5}$$

where $\overline{\eta^2}$ denotes the mean square value of E(t).

The cumulative probability distribution function of E(t) is by eq. (1.12):

$$Q_E(\eta) = 1 - e^{\frac{\eta^2}{\overline{\eta^2}}} \tag{2.6}$$

The average value of the $1/n$ higher values of E(t) denoted by $\overline{\eta}^{(1/n)}$ is given by:

$$\overline{\eta}^{(1/n)} = \frac{\int_{\eta^*}^{\infty} P_E(\eta)\,\eta\, d\eta}{\int_{\eta^*}^{\infty} P_E(\eta)\, d\eta} \tag{2.7}*$$

where η^* is defined by the relation:

$$1/n = 1 - Q_E(\eta^*) \tag{2.8}$$

*The relation (2.7) gives the values of $\overline{\eta}^{(1/n)}$ for any probability density function

Geometrically, Fig. (3), the value

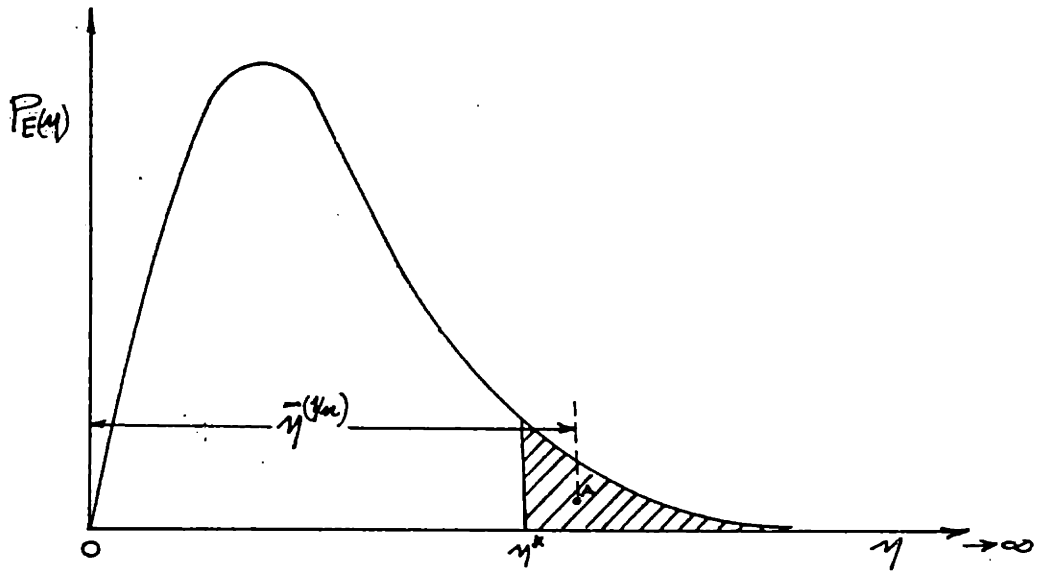

Figure (3)

of $\bar{\eta}^{(1/n)}$ can be conceived as the distance of the centroid, of the shaded area, A from the axis of $P_{E(\eta)}$.

By (1.12) and (1.13) the relation (2.7) becomes:

$$\bar{\eta}^{(1/n)} = e^{\frac{\eta^2}{\bar{\eta}^2}} \int_{\eta^*}^{\infty} \frac{2}{\bar{\eta}^2} e^{(-\eta^2/\bar{\eta}^2)} \eta \, d\eta$$

or

$$e^{-\eta^2/\bar{\eta}^2} \bar{\eta}^{(1/n)} = -\int_{\eta^*}^{\infty} \eta \, d e^{-\eta^2/\bar{\eta}^2}$$

After integrating the right hand by parts and dividing the relation by $\bar{\eta}^2 \, \& \, e^{-\eta^2/\bar{\eta}^2}$ we get, since $\eta^* = [\bar{\eta}^2 \log n]^{1/2}$ (2.8),

$$\frac{\bar{\eta}^{(1/n)}}{\bar{\eta}^2} = (\log n)^{1/2} + \frac{n\sqrt{\pi}}{2}\left[1 - H\{(\log n)^{1/2}\}\right] \qquad (2.9)$$

where $H(\theta) = \frac{2}{\sqrt{\pi}} \int_0^{\theta} e^{-\theta^2} d\theta$ the error function.

The above result can be found in [3] and the values of $\frac{\bar{\eta}^{(1/n)}}{\bar{\eta}^2}$ are tabulated for values of n up to 100.

Since the error function is a tabulated one we proceed the tabulating for values of n up to 10^9, [9], and the results appear in Table 1.

Table 1

Representative values of $\frac{\bar{\eta}^{(1/n)}}{\bar{\eta}^2}$ for a Rayleigh distributed random variable

n	$\frac{\bar{\eta}^{(1/n)}}{\bar{\eta}^2}$	n	$\frac{\bar{\eta}^{(1/n)}}{\bar{\eta}^2}$
1	0.886	20	1.986
2	1.256	10^2	2.359
3	1.416	10^3	2.795
4	1.517	10^4	3.041
5	0.591	10^6	3.722
10	1.800	10^9	4.553

From eq. (2.9) we see that since $H(\theta) \longrightarrow 1$ for values of θ larger than 3, i.e. $n \approx 1000$, the ratio $\frac{\bar{\eta}^{(1/n)}}{\bar{\eta}^2} \longrightarrow \infty$ logarithmically as $n \to \infty$.

2.3 The general case of the statistical distribution of the maxima of a random process

In ref. [4] we find that the probability density function of the maxima of a random process is given by:

$$P_{max.f}(\eta) = \frac{1}{\sqrt{2\pi}}\left[\varepsilon e^{-\frac{1}{2}\eta^2/\varepsilon^2} + (1-\varepsilon^2)\eta e^{-\frac{1}{2}\eta^2}\int_{-\infty}^{\frac{\eta(1-\varepsilon^2)^{1/2}}{\varepsilon}} e^{-\frac{1}{2}x^2}\,dx\right] \qquad (2.10)$$

where ε = the broadness factor and $\eta = \frac{\xi}{m_o^{1/2}}$ (2.11)

In (2.11) ξ denotes the maximum values of the departures of f(t) from the mean level and can be both positive and negative; m_o is the zero moment of the spectrum of f(t).

The limiting forms of the above expression are 1) the Gaussian distribution as $\varepsilon \to 1$ with probability density function

$$P_{\xi}(\xi) = \frac{1}{\sqrt{2\pi m_o}}\, e^{-\xi^2/2m_o}, \quad -\infty \le \xi \le \infty \qquad (2.12)$$

and 2) the Rayleigh distribution as $\varepsilon \to 0$ with probability density function

$$P_{\Xi}(\xi) = \begin{cases} \frac{\xi}{m_0} e^{-\xi^2/2m_0} & \xi \geq 0 \\ 0 & \xi < 0 \end{cases} \qquad (2.13)$$

3. APPLICATION OF THE STATISTICAL RESULTS TO THE SEA WAVE FORM AND TO SHIP RESPONSES

3.1 The Statistical distribution of the maxima of the sea waves and ship responses

The Rayleigh distribution function has been extensively used by oceanographers and naval architects to describe the distribution of the maxima of the wave system and of the ship responses and relatively good agreement was found between theory and, both full scale and model scale, experiment.

Nevertheless, the application of the Rayleigh distribution for the maxima of a random process as defined in the literature of the conducted experiments, see [6] and[7] for example, is an approximation for several reasons as explained in the following.

3.2 The approximation of the Rayleigh distribution

The Rayleigh distribution hold for the envelope of a narrow band process. This envelope is symmetrical about the mean level line and therefore the distribution holds for the half width of the envelope, too. Buththe apparent heights of process as usually defined (the distance between a crest of the preceeding or following trough) do not coincide with the width of the envelope nor do the amplitudes coincide with the half width of the envelope (see Fig. (4)).

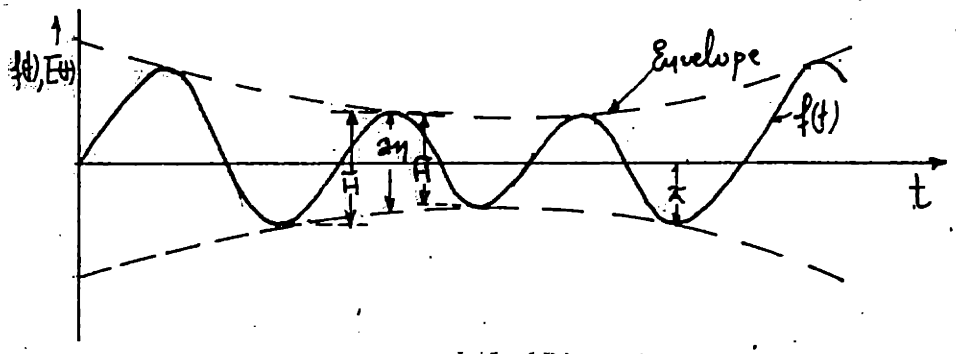

Figure (4)

Even if we assume that the maxima of the process occur very nearly on the envelope, we have to assume additionally that $|\tilde{A}_{ci}| = |\tilde{A}_{\tau i}|$ or that the envelope of the process is very slowly changing with time. From records of the seaway and ship responses (see Fig. (5)), we see that the above assumption is not justified for most of the cases.

An additional statistical reason that the Rayleigh distribution is only an approximation is that the sampling from the population of the envelope values is not random but has to be taken from the population of the maxima of the process which coincides with the envelope at some instances only.

The above limitations apply to the case of an ideally narrow-band process. The sea wave form and the ship responses are not ideal narrow band processes, can be of the wide band type (e.g. the wave form) and therefore the Rayleigh distribution is for another reason not scientifically justified for the maxima of the wave form and ship responses (defined as the distance between a crest and a trough).

Nevertheless, analysis of both full scale and model scale data to a moderate extent (see [6] and [7]) has shown considerable agreement with the Rayleigh distribution. This can be justified as follows:

a) Pitching and Heaving Motions - The pitch and heave response of the filter are very nearly narrow band processes. This can be shown from Fig. (5) which is a typical part of a model scale record of pitching and heaving motions. The almost total absence of ripples suggest that according to the relation 1.7, $\varepsilon \to 0$. Also a symmetrical envelope can be plotted for these processes.

Moreover, several investigations have shown that the departure from the zero mean level of the wave form is a Gaussian distributed random process. Thus, assuming that the ship acts like a linear time invariant filter, the

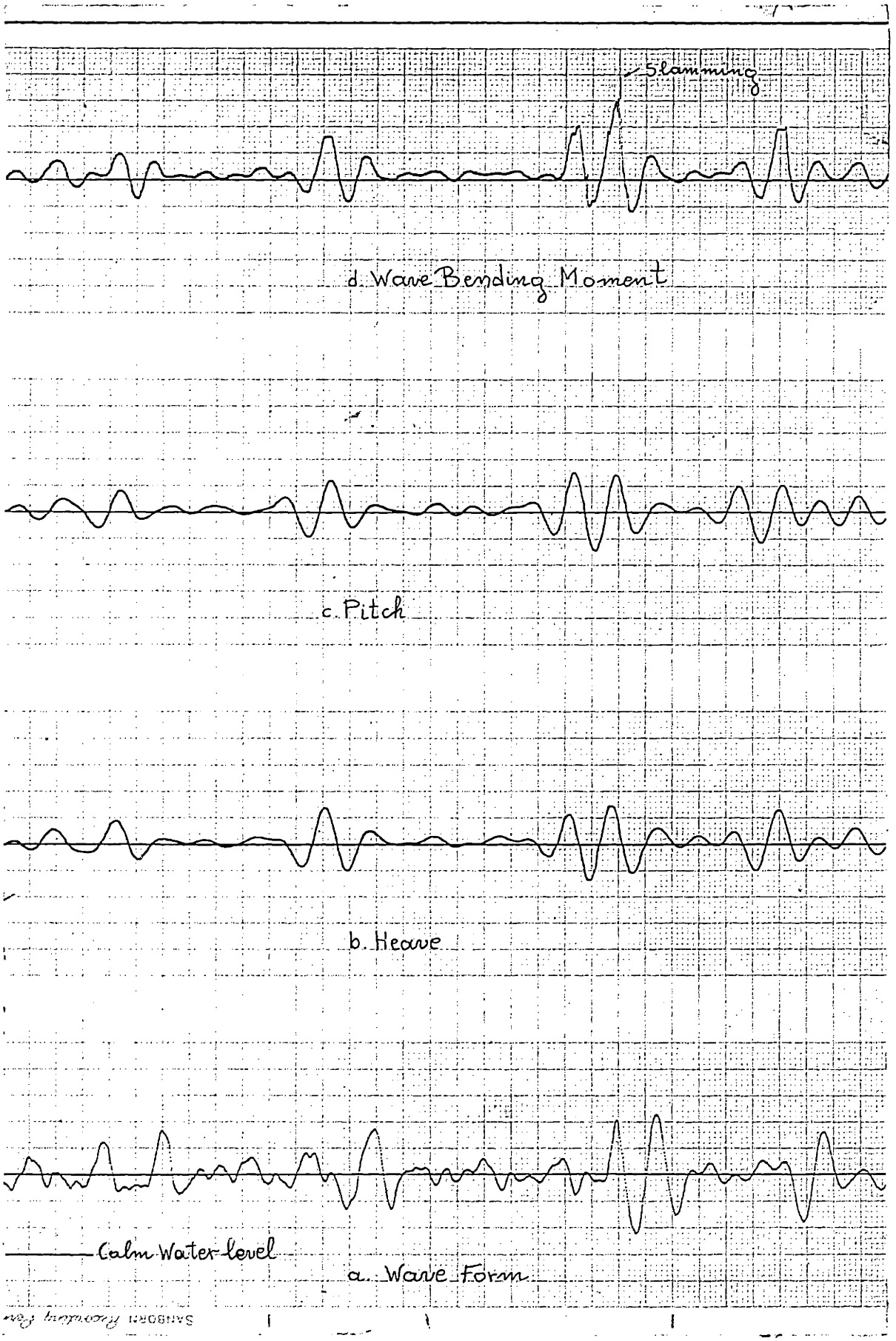

FIG. 5a

WHITE NOISE WAVE FORM & SHIP RESPONSES

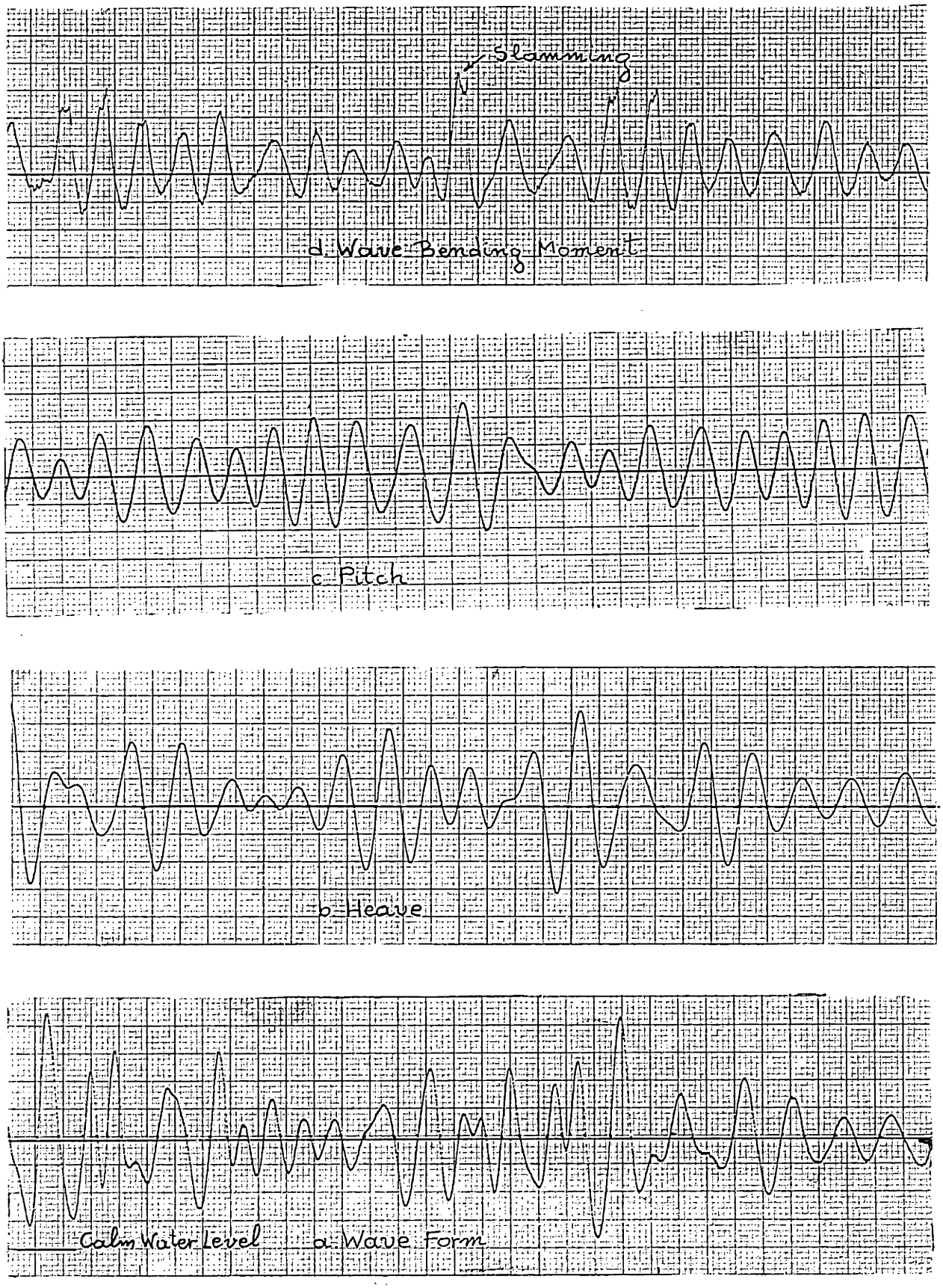

FIG. 5b

SINE WAVE COMPONENTS WAVE FORM & SHIP RESPONSES

ship responses are Gaussian distributed too. Here we have to add that the departures of the heave and pitch records are not taken from the calm water level but from the actual mean of the process which is shown to be different (see [10]), and therefore the requirement of a zero mean process is satisfied.

Given the above conditions the only discrepency that remains, so that the application of the Rayleigh distribution to the distance between a crest and a trough for the pitching and heaving motions is scientifically justified, is the distinction between apparent height and envelope width. The results seem to prove that the above approximation does not lead to serious differences.

b) Wave form - Examination of actual and model scale wave records shows (see Fig. (15), part A and Fig. (5)) that a large number of ripples is present. Therefore we cannot assume $\varepsilon \to 0$ and the broadness factor lies somewhere between 0 and 1. The upper limit according to the relation 1.7 means that an infinite number of small amplitude ripples are superimposed to a carrier wave and the distribution of the maxima tends to the limit to the distribution of the carrier wave, i.e. the Gaussian distribution.

For some wave records ε has found to be in the range $.57 < \varepsilon < .67$ [4] .

Therefore the only possible explanation for the good results found in the literature is that by neglecting ripples (and that is exactly what we are doing by the definition of apparent heights), we transform the wave form to a narrow band process.

c) Longitudinal wave bending moment - The above random process which is superimposed to the calm water bending moment has also been examined for

the statistical distribution of its apparent heights.

Typical records of the process (see Fig. (5)) show that 1) it is not a wide band process if we judge from the number of ripples, 2) its mean departs a great deal from the still water level and 3) the process possesses apparent irregularities caused by slamming.

Therefore, the maxima of the process can be examined for Rayleigh distribution only if we neglect ripples, if we take the actual mean level to measure departure to satisfy the Gaussian distribution of process requirements, and if we neglect the slamming effects. The last condition is difficult to satisfy because of the uncertainty of where the effects of slamming start and the process stops.

4. EXPERIMENTAL PROCEDURE AND RESULTS

4.1 Ship and Sea Models

The ship tested in irregular seas was a 1/96 scale ratio of a high speed cargo ship of the Racer type with full scale hull particulars as in Table 2.

Table 2

Full Scale Hull Particulars

Length between perpendiculars	507 ft.
Breadth	75 ft.
Depth	42.5 ft.
Draft	27 ft.
C_b	0.578 ft.
LCB (aft ℄)	6.15 ft.
LCF (aft ℄)	14.2 ft.
Radius of gyration (0.25 LBP)	127 ft.
Displacement	16,925 L.T.

The full scale spectral densities of the sea state in which the model was tested appear in Fig. (6).

Wave 2 and Wave 3 are white noise generated models (see Part A), whereas Wave 1 is a sine wave components model.

The ship speed was 19.7 knots for waves 1 and 2 and 14.7 knots for wave 3.

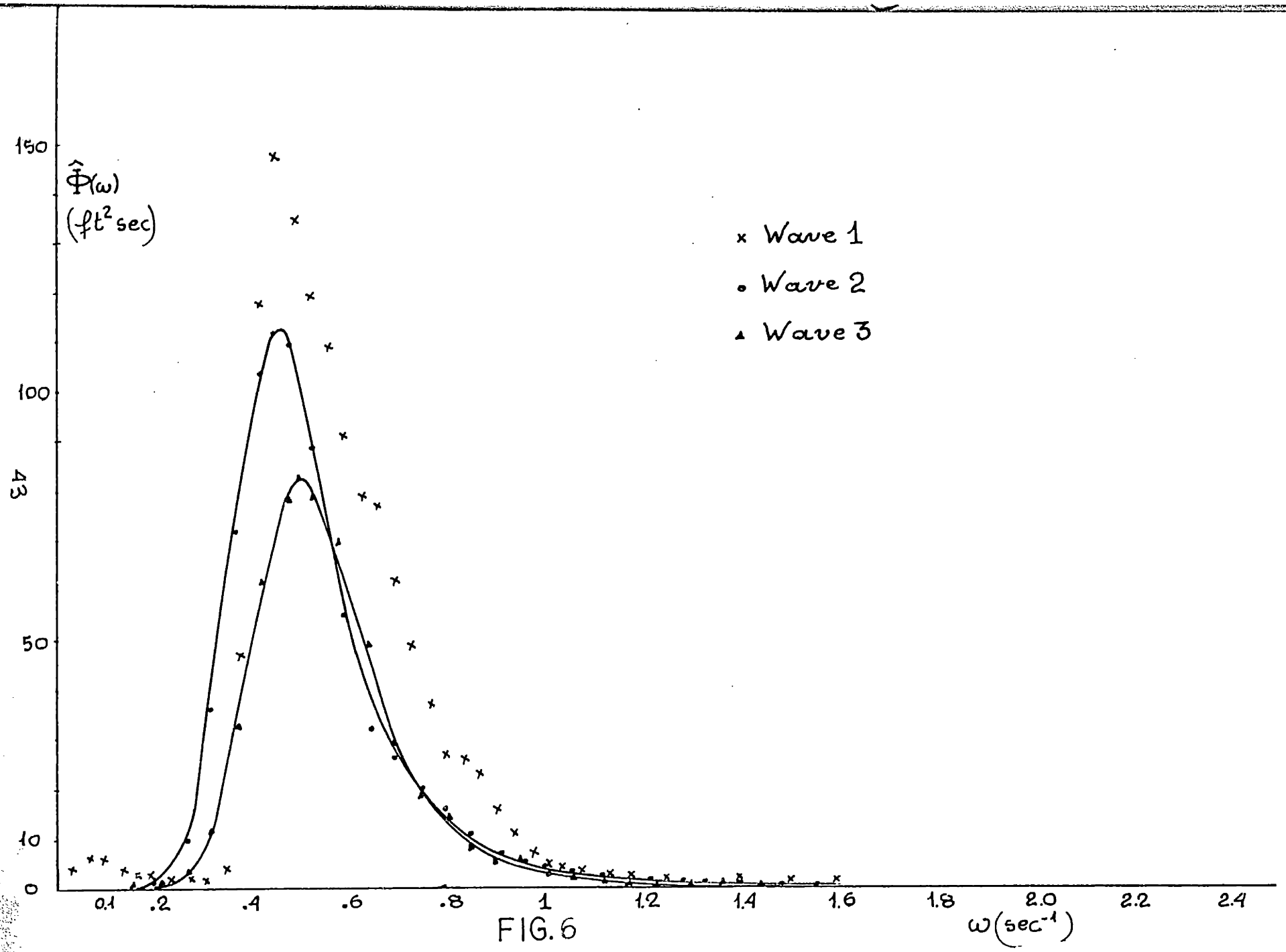
150
100
50
10
0
$\hat{\Phi}(\omega)$
$(ft^2 sec)$
× Wave 1
• Wave 2
▲ Wave 3
0.1
.2
.4
.6
.8
1
1.2
1.4
1.6
1.8
2.0
2.2
2.4
$\omega(sec^{-1})$

FIG. 6

4.2 Measurements and Process of the Data

The experiments were performed at the Ship Model Towing Tank at Massachusetts Institute of Technology.

Wave form, pitch, heave and longitudinal wave bending moment were recorded on tape and paper (see Figures (5a) and (5b)).

The wave form was measured with a sonic wave probe at point 1 ft. 3 in. in front and 1 ft. 6 in. sideways of the model.

The ship responses were measured amidships with differential transducers.

The data tape was digitized with the analog to digital conversion computer program of the Department of Naval Architecture and Marine Engineering, and the digitized data was processed for results with a special written computer program.

Both of the above processes were performed at the Computation Center at Massachusetts Institute of Technology. Since the length of the towing tank was not adequate to give enough data in one run, the results of several consecutive runs were used, provided that the wave command signal tape was long enough to cover all the runs without being repeated.

The number of full cycles recorded was of the order of 500 for wave 1, 1000 for wave 2 and 750 for wave 3; by "full cycle" we denote the distance between two zero up crossings.

The digitizing rate for all cases was 10 points per second.

4.3 Description of the Computer Program

In order to improve the approximation of the Rayleigh distribution of the apparent heights of the different processes a new definition of the wave height was used (see Fig. 7).

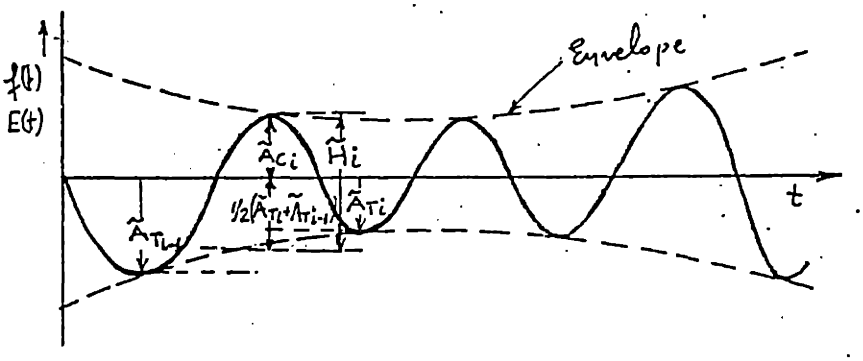

Figure (7)

Definition of the Apparent Height

As we see the apparent height is defined as:

$$\tilde{H}_i = \tilde{A}_{ci} + \tfrac{1}{2}\left(\tilde{A}_{\tau i-1} + \tilde{A}_{\tau i}\right) \qquad (4.1)$$

The reason for the above definition is that in so doing we are more close to the width of the envelope than if we use the common definition which defines:

$$\tilde{H}_i = \tilde{A}_{ci} + \tilde{A}_{\tau i-1} \text{ or } \tilde{H}_i = \tilde{A}_{ci} + \tilde{A}_{\tau i} \qquad (4.2)$$

As we have seen before, the Rayleigh distribution holds for the width of the envelope of a narrow ban process and this is different than $\tilde{H}_i$ as defined in 4.2.

Strictly speaking (4.1) is also an approximation of the width of the width of the envelope but much more accurate than (4.2), especially if the width of the envelope is relatively rapidly changing.

The computer program accepts as input data the digital representation of the process measured, in integer form, with values from 0 - 1000, from 0 as a base line.

The program calculates the mean of the process and by subtracting the mean from the input data calculates the departures - positive or negative - from the mean level.

 (pg. 46 does not exist)

Then the program searches for and spots the crests and troughs of the process as defined in Fig. (1) (one crest and one trough between two zero up crossings. The ripples are neglected.)

The next step is the calculation of the apparent heights as defined in (4.1) and their ordering in decreasing order.

Assuming that we have N + 1/2 full cycles and, therefore, N + 1 crests, N troughs and N apparent heights, (the program neglects the data before the first and after the last crest) the root mean square value of the wave heights is given by:

$$\tilde{H}_{R.M.S.} = \left(\frac{1}{N} \sum_{i=1}^{N} \tilde{H}_i \right)^{1/2} \qquad (4.3)$$

The average of the $1/n = P$ highest apparent heights is calculated (the apparent heights being in decreasing order) by:

$$\tilde{H}^{(P)} = {}^{n}/_{N} \sum_{i=1}^{N/n} \tilde{H}_i \qquad (4.4)$$

The final output of the program are the ratios $\tilde{H}^{(P)}/\tilde{H}_{R.M.S}$. The values of p are in the range 1 - 0.002 for this program but the range can be changed according to the length of the data.

All four processes were analyzed by the same program and in the case of bending moment the slamming effects were included in the analysis.

The results appear in Figs. (8), (9), (10), and (11) where the ratios $\tilde{H}^{(P)}/\tilde{H}_{RMS}$ are plotted against the theoretical relation given by 2.9 for pitch, heave, wave form and longitudinal wave bending moment.

4.4 Discussion of the Results

As has been mentioned before the main scope of this investigation was the detection of the range where nature imposes a cut-off to the values of the 1/n highest apparent heights of the wave form and the ship responses which, naturally, do not tend to infinity as $\frac{1}{n}$ tends to zero, as the

theoretical relation 2.9 suggests. In fact, nature, i.e. the instability of the crests of the waves, restricts the heights of the wave form and since this is the input to the ship system a cut-off of the ship responses follows.

The fact that the apparent heights of the wave form and the ship responses follow the Rayleigh distribution up to a certain limit would be a "by product" of the investigation.

In fact, from Figs. (8), (9), (10), and (11), we see that, up to the 1/20 higher apparent heights, all the cases examined do follow very closely the theoretical distribution as many other experimental results did in the past. From the above figures we note that the agreement is really astonishing for values of 1/n up to 1/3 (the significant apparent heights) if we keep in mind the many approximations that separate the theoretical distribution of the width of the envelope of an ideal narrow band process from the distribution of the apparent heights of our processes.

For values of 1/n smaller than 1/20 we have to examine each case separately. Unfortunately, the length of the experiments required to obtain long enough data, which suits the needs of this investigation, is such that only three cases have been studied. Furthermore, we have to distinguish the three cases from each other because wave 2 and wave 3 are both of the white noise type, but with different speeds, and wave 1 is of the sine wave components type.

The conclusions that can be derived from the examination of Figs. (8), (9), (10) and (11) are the following:

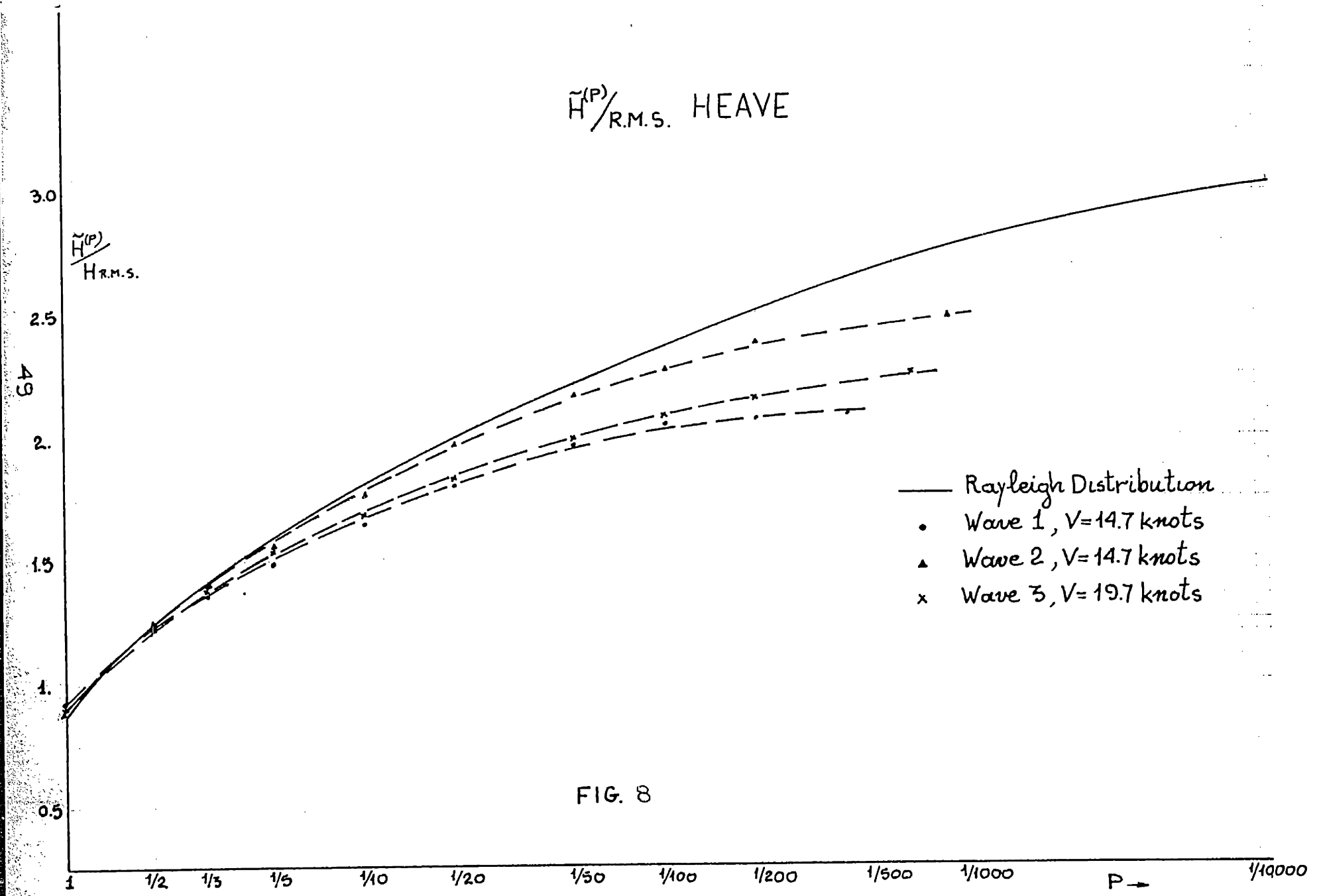
$\tilde{H}^{(P)}/_{R.M.S.}$ HEAVE
3.0
$\tilde{H}^{(P)}/H_{R.M.S.}$
2.5
2.
1.5
1.
0.5
49
1
1/2
1/3
1/5
1/10
1/20
1/50
1/100
1/200
1/500
1/1000
P →
1/10000
Rayleigh Distribution
Wave 1, V=14.7 knots
Wave 2, V=14.7 knots
Wave 3, V=19.7 knots

FIG. 8

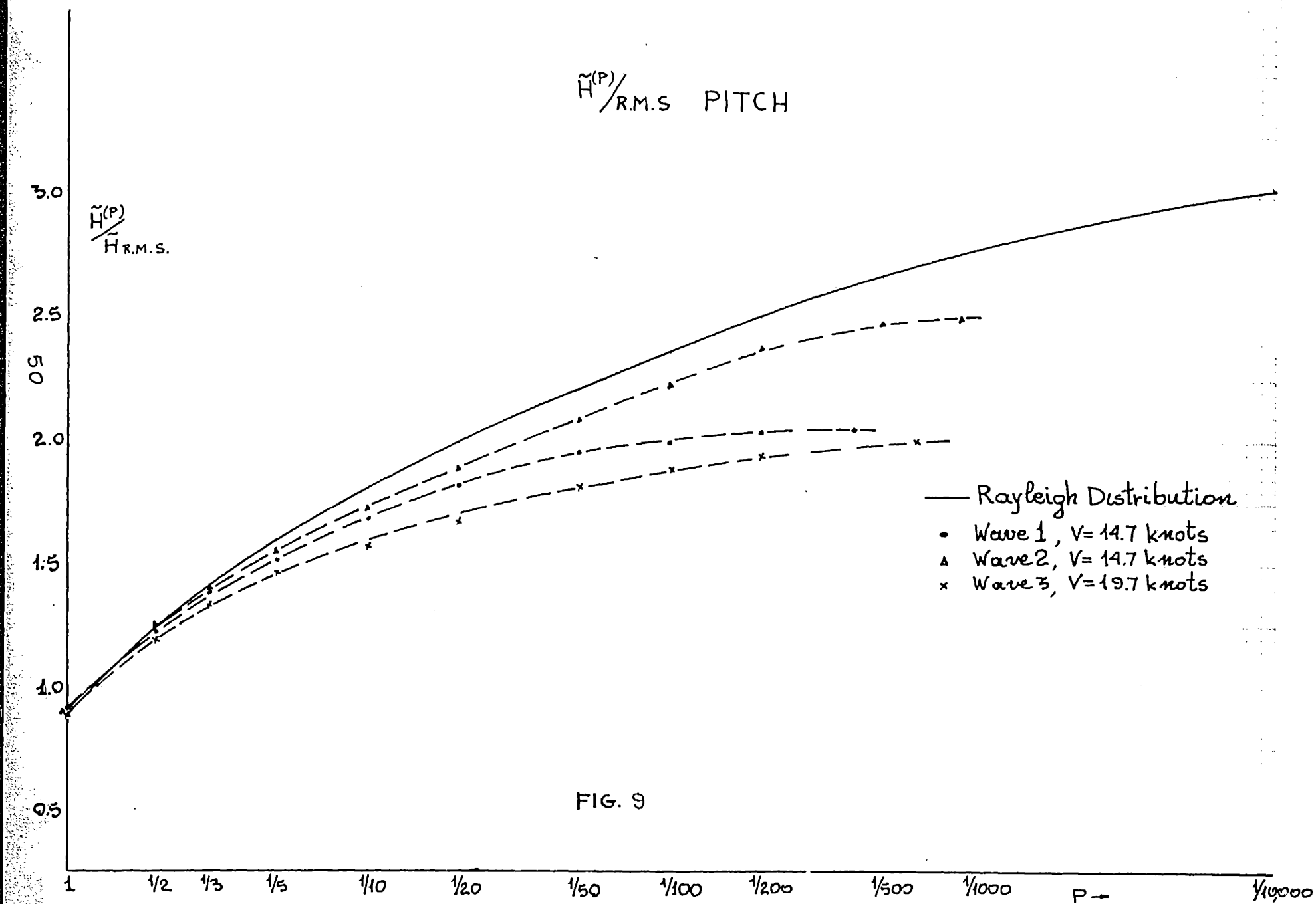
$\tilde{H}^{(P)}/_{R.M.S}$ PITCH
$\tilde{H}^{(P)}/\tilde{H}_{R.M.S.}$
3.0
2.5
2.0
1.5
1.0
0.5
SO
Rayleigh Distribution
Wave 1, V= 14.7 knots
Wave 2, V= 14.7 knots
Wave 3, V= 19.7 knots
1
1/2
1/3
1/5
1/10
1/20
1/50
1/100
1/200
1/500
1/1000
P →
1/10000

FIG. 9

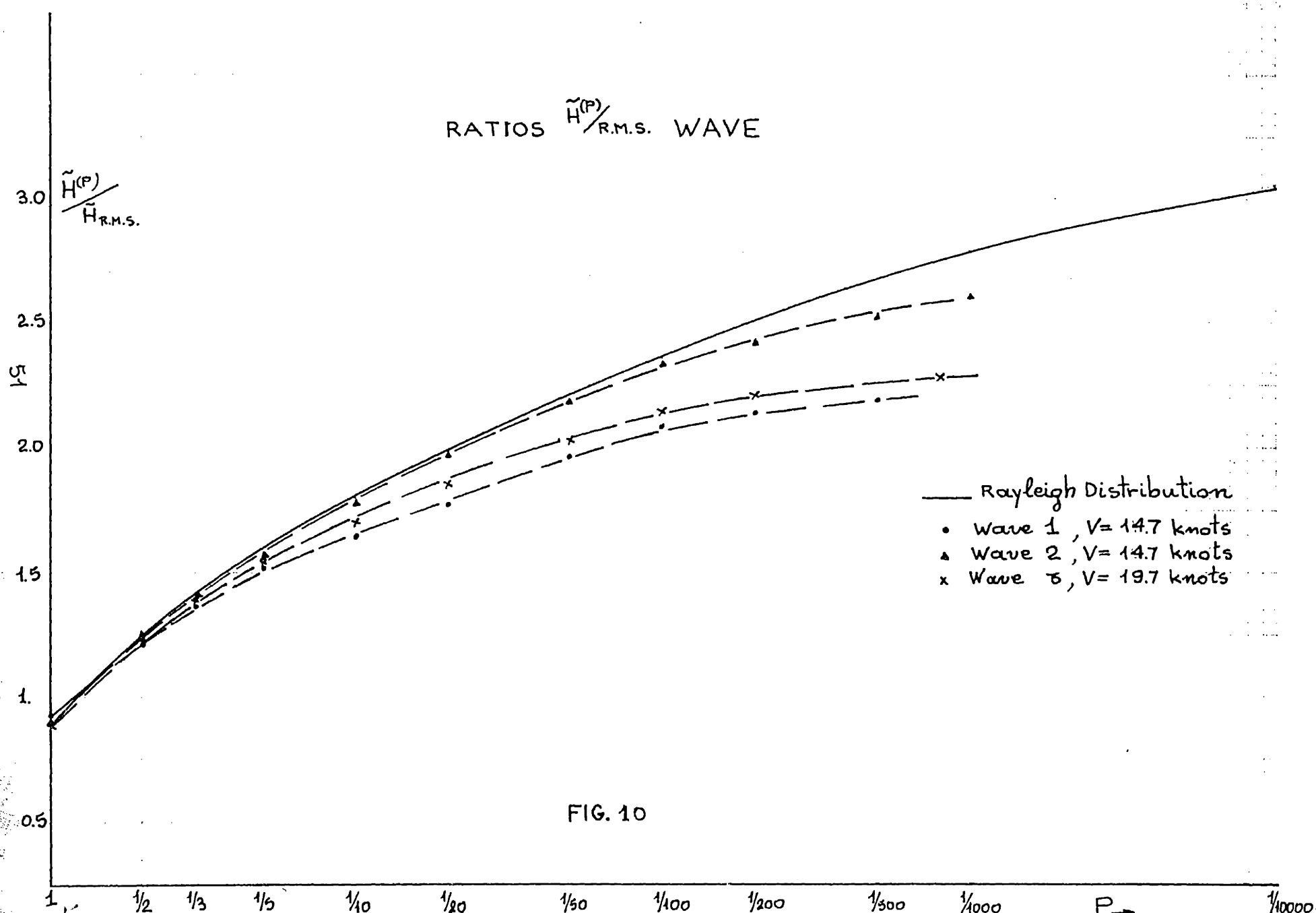
RATIOS $\tilde{H}^{(P)}/_{R.M.S.}$ WAVE
$\tilde{H}^{(P)}/\tilde{H}_{R.M.S.}$
3.0
2.5
2.0
1.5
1.
0.5
5.1
Rayleigh Distribution
Wave 1 , V= 14.7 knots
Wave 2 , V= 14.7 knots
Wave 3 , V= 19.7 knots
1
1/2
1/3
1/5
1/10
1/20
1/50
1/100
1/200
1/500
1/1000
1/10000
P

FIG. 10

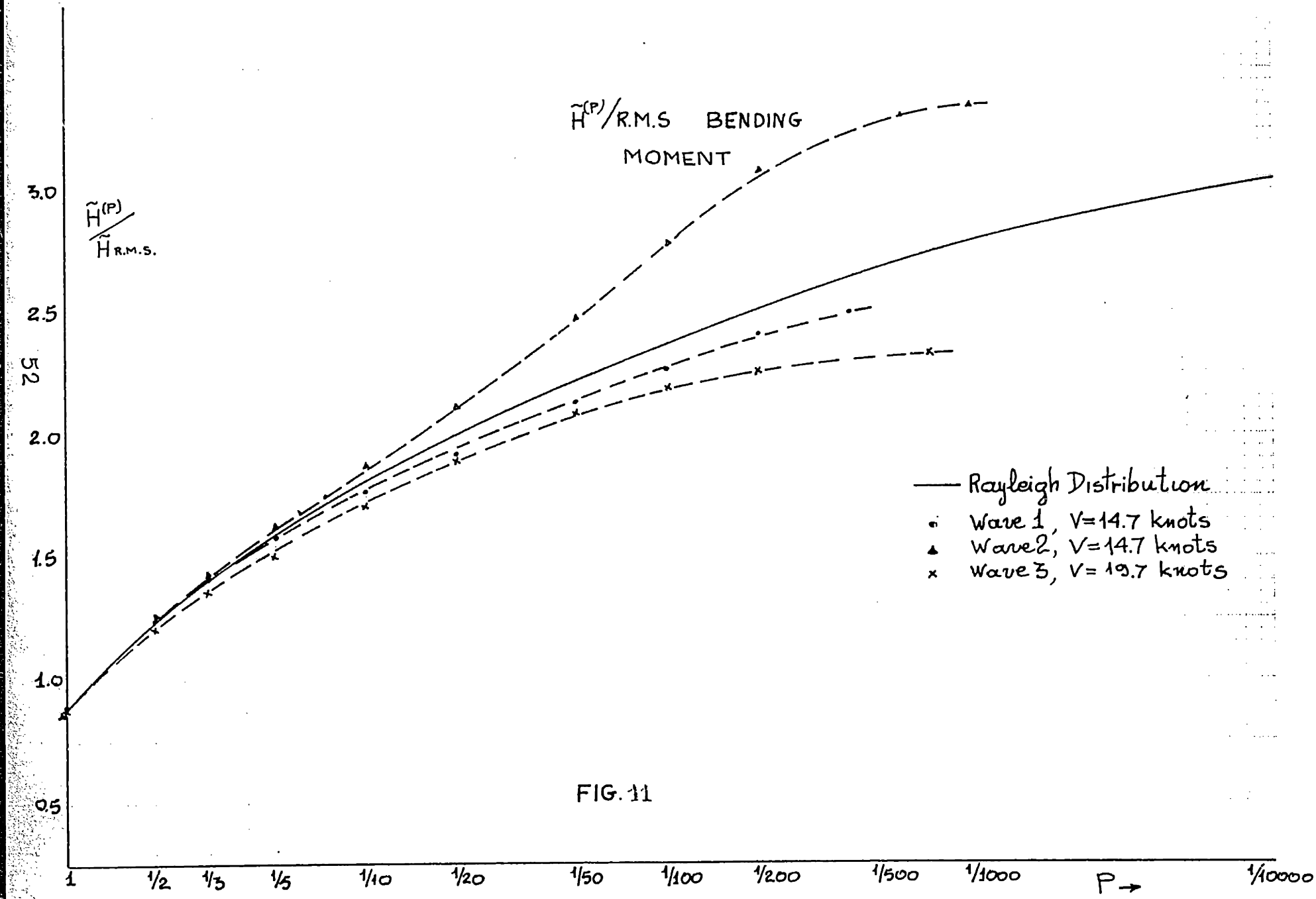
$\tilde{H}^{(P)}$/R.M.S BENDING MOMENT
$\frac{\tilde{H}^{(P)}}{\tilde{H}_{R.M.S.}}$
3.0
2.5
2.0
1.5
1.0
0.5
Rayleigh Distribution
Wave 1, V=14.7 knots
Wave 2, V=14.7 knots
Wave 3, V=19.7 knots
1
1/2
1/3
1/5
1/10
1/20
1/50
1/100
1/200
1/500
1/1000
1/10000
P →

FIG. 11

a) Waves 2 and 3. Both are waves generated with the white noise procedure. From Fig. (6) we see that wave 2 corresponds to higher seas, but both do not include apparently breaking crests (whitecaps).

a1) Pitch and Heave - From Figs. (8) and (9) we see that the responses to wave 2 are more close to the Rayleigh distribution. A possible explanation to the above difference is that although the less severe seas with less wave crest instabilities should follow better the Rayleigh distribution, the effect of the higher speed is such that reverses the trend.

The heaving and pitching motions are the more close approximations to the ideal narrow band model. With the low speed both responses do follow very closely the theoretical distribution up to $1/n = 1/200$ and then tend to level off with values of $\tilde{H}^{(P)}/\tilde{H}_{R.M.S}$ very close to 2.5. With the higher speed the responses follow the theoretical distribution up to $1/n = 1/100$ and then depart reaching a limiting value of $\tilde{H}^{(P)}/\tilde{H}_{R.M.S.}$ close to 2.05.

a2) Wave Form - From Fig. (10) we see that, similarly as for pitch and heave, the apparent heights of the wave that corresponds to the lower ship speed and higher seas follow more closely the theoretical distribution.

Here the aforementioned explanation of the speed effect does not hold since the wave heights are independent of the ship speed. The only possible explanation of this difference is that, the wave form being a rather wide band process, the digitizing rate of 10 points per second was not adequate for the higher speed that causes larger frequencies of encounter.

From Fig. (10) we also see that the values of $\tilde{H}^{(P)}/\tilde{H}_{R.M.S}$ follow the theoretical

distribution for values of 1/n up to 1/100 and then tend to a limiting value of 2.6. For wave 3 the corresponding values are 1/n ~ 1/50 and $\tilde{H}^{(P)}/\tilde{H}_{R.M.S} = 2.2$. For all cases, including the corresponding to wave 1, we see that the wave form follows more closely the theoretical curve and levels off for smaller values of 1/n, with larger limiting values of $\tilde{H}^{(P)}/\tilde{H}_{R.M.S.}$, than the pitch and heave responses.

a3) Longitudinal Wave Bending Moment - As was mentioned before the due to slamming peaks were included in the analysis.

From Fig. (11) we see that there is a striking difference in the ship response to waves 2 and 3.

For wave 3 the lower seas and higher speed with the low digitizing rate made the process behave like a narrow band process that levels off for values of $1/n \ll 1/100$ with limiting value $\tilde{H}^{(P)}/\tilde{H}_{R.M.S.} = 2.1$.

This is not the case for the ship response to wave 1. Here the effect of slamming is apparent and we cannot say anything about limiting value of $\tilde{H}^{(P)}/\tilde{H}_{R.M.S}$. Nevertheless, for values of 1/n up to 1/10 we see that the effects of slamming are diminished by averaging and that the process follows very closely the theoretical distribution.

In any case, the analysis of the wave bending moment process is the more difficult and can lead to erroneous results as far as the smaller values of 1/n are concerned. In fact, from Figures (5) and (5a) we see that any practical digitizing rate can miss some of the impulse-like maxima due to slamming.

b) Wave 1. From Figs.(5a) and (5b) we can distinguish the difference in the wave form of the sine wave components type and the white noise type, although both are assumed to possess spectral densities of the

Pierson-Moskowitz form.

From Fig. (6) we see that wave 1 corresponds to higher seas than wave 2 and breaking crests were present during the experiments.

From Figs. (8), (9), (10), and (11) we see that the wave form and ship responses for wave 1 lie below the corresponding curves for wave 2.

This can be explained since the ship speed was the same by the expected effect of the breaking crests of wave 1. Also, from Figs. (5a) and (5b) we see that from the point of view of number of ripples the sine wave components wave form is more of the narrow band type than the white noise wave. When examining the white noise wave form and whip responses we had noticed that, under the present analysis, the more wide banded wave form did follow more closely the theoretical curve. This trend is repeated here for the two wave forms.

From Fig. (8) and (9) we see that the heave, pitch curves of $\tilde{H}^{(P)}/\tilde{H}_{R.M.S.}$ follow the Rayleigh distribution for values of 1/n up to 1/100 and then level off with limiting value 2.1.

The corresponding values for the wave form are $1/n \simeq 1/100$ and $\tilde{H}^{(P)}/\tilde{H}_{R.M.S} =$ 2.25 (Fig. 10). The bending moment curve seems to follow the theoretical curve as far as the length of the data permits the analysis to be extended. The dissimilarity of the bending moment curves for wave 1 and wave 2 is strange at first sight and since wave 1 corresponds to higher seas at the same speed the trend should be the opposite.

The explanation of this phenomenon is apparent when one examines the bending moment processes in Figs. (5a) and (5b). We see that the level of the peaks due to slamming in the case of the white noise wave form is much greater than the level of the ordinary peaks. This difference is much reduced in the case of the sine wave components wave and thus the behavior of the ratios $\tilde{H}^{(P)}/\tilde{H}_{R.M.S.}$ in Fig. 11 agrees with the time history of the processes.

From the above results we see that the expected cut-off of the apparent heights for wave form, pitch and heave occurs for values of 1/n smaller than 1/50 to 1/100 and that the limiting values of $\tilde{H}^{(P)}/\tilde{H}_{R.M.S}$ are affected by the ship speed and the type of the wave form. The higher speed tends to lower the limiting value of $\tilde{H}^{(P)}/\tilde{H}_{R.M.S.}$ for the pitch and heave responses.

For the bending moment case we can say that although the process seems to follow the Rayleigh distribution for values of 1/n up to 1/10, for smaller values of 1/n the effects of slamming make the digitized data unreliable and the notion of a cut-off meaningless for the cases where enough slamming is present.

4.4 Possible extensions of the present investigation

It has been stressed many times during the development of this thesis that the Rayleigh distribution of the probability density function of the apparent heights of the wave form and the various ship responses is only an approximation.

Therefore one can argue that it would be better to apply rigorously the probability density function given by the relation 2.10 to the stationary points of a random process.

The opinion of the author is that the application of the relation 2.10 is not practical for seakeeping application for the following reasons:

a) The probability distribution function of 2.10 refers to the variable $\eta = \frac{\xi}{m_0^{1/2}}$. Therefore, to obtain the variable η one needs, on the one hand the spectral density function of the process and on the other hand the mean level of the process from which point the maxima of elevations are measured.

For seakeeping applications the spectral density function of a process and its mean level are not always easily obtained. Furthermore, the values of ξ are restricted to maxima or minima and they can be positive or negative corresponding for example to above or below the mean level maxima. The intuition of the seafarer is not and cannot be correlated to such a variable as ξ and the notion of, for example, the maximum possible heave maximum above the mean level is irrelevant if we do not know what is the value of the preceeding or following heave minimum.

We have to add to the above that the experimental determination of ξ is very difficult. Whenever long data is required, as it is usually the case in statistical applications, processing of the data by any other means than analog to digital machine conversion becomes impractical. But if we have to detect the ripples of a process, any small and otherwise negligible oscillation of any of the electronic instruments used to record, reproduce, amplify and digitize the data would add ripples and thus values of to process and thus leading to erroneous results.

b. The attempt of determining a correction factor based on 2.10 with which one can multiply the values of $\tilde{H}^{(P)}/\tilde{H}_{R.M.S}$ that appear in Table(1) in case of $\varepsilon \neq 0$ does not lead to meaningful results. In Ref. [11] we find a definition of the correction factor as $(1-\varepsilon^2)^{1/2}$. But even if the ordinates of the graph of p.73 that gives $\tilde{H}^{(P)}/\tilde{H}_{R.M.S}$ as a function of ε will be divided by a factor $\sqrt{\frac{\pi}{2}}$ as appears correct (see Ref. [12]) the results do not agree. For example, for 1/n = 1/10 and $\varepsilon = 0$ from Table 1 we have $\tilde{H}^{(1/10)}/\tilde{H}_{R.M.S} = 1.800$ and from the above figure:

$$\frac{\tilde{H}^{(1/10)}}{\tilde{H}_{R.M.S}} = \frac{2.6}{\sqrt{\pi/2}} = 2.080$$

The above disagreement occurs despite the fact that relation 2.10 tends

to the limit as $\varepsilon \to 0$ to the proper Rayleigh distribution (see (2.5) and (2.12)).

For values of $\varepsilon \neq 0$, if $\tilde{H}$ is defined as defined as usual in seakeeping work or as in the present thesis, it is misleading to take into account a correction factor based on the broadness factor ε and thus on the higher frequencies of the spectral density when by the definition of the higher frequencies have been neglected.

Therefore, it seems much more safe and practical to continue working with apparent heights, especially if they are defined as in the present thesis. The analysis of experimental data justifies the approximation made and the data is much more easily proceeded.

The above discussion holds mainly for the wave form and wave bending moment processes. The pitch and heave processes are of the narrow band type and therefore the Rayleigh distribution can be applied with confidence.

The results of the present investigation did not show a clear-cut cut-off in the values of $\tilde{H}^{(P)}/\tilde{H}_{R.M.S}$ for small values of $1/m$. It is apparent that more data is required, possibly up to 3000 - 4000 full cycles.

The above number of cycles corresponds to several hours of full scale trials. Since the meteorological conditions and hence the sea spectrum are not likely to remain constant for such a long period, the only place at which these experiments can be conducted is the model ship towing tank.

Since, as it is shown in Part A of this thesis, the sea state model can be a very accurate representation of the real sea. At least with the model of the real sea that the state of the art of Oceanography can provide the results are expected to give a real image of the full scale situation.

When the cut-off of the values of $\tilde{H}^{(P)}/\tilde{H}_{RMS}$ is found experimentally with the effects of speed, sea condition and hull dimensions and form incorporated in the final result, the practical importance becomes evident.

The Naval Architect will be able to predict the probable maximum expected apparent heights of the wave form and the ship responses as a function of the ship, the ship's speed and the possible sea states the ship is going to encounter. The above can be predicted by tank tests long enough to give the $\tilde{H}_{RMS}$ of the process or by the use of the ship response operators (frequency responses) as follows:

From equation (2.4) we see that:

$$\tilde{H}_{R.M.S} = 2m_o \qquad (4.5)$$

From relations (2.5) and (4.5) we see that the Rayleigh probability density distribution for the case of apparent heights can be written as:

$$P_{\tilde{H}}(h) = \frac{h}{2m_o} e^{-h^2/8m_o}, \quad 0 \le h \le \infty \qquad (4.6)$$

Where h the experimental value of $\tilde{H}$ and $h = 2\eta$

The above result holds for ideal narrow band processes only and can be applied, subject to experimental verification, to the pitching and heaving motions.

Therefore, for pitching and heaving motions, if we assume the sea state and the ship response operators given, we can find the pitching and heaving spectra. Hence, having m_o we can predict the limiting values of $\frac{\tilde{H}^{(P)}}{\tilde{H}_{R.M.S}} = \tilde{H}^{(P)}/2m_o$ without specific experiments.

For wave form and wave bending moment, equation (4.5) must be verified experimentally and a correction, if any, be made to the constant. Then the same procedure as above can be followed.

LIST OF REFERENCES

PART B

1. Rice, S. O., "Mathematical Analysis of Random Noise," Bell System Technical Journal, Vol. 24.
2. Parzen, E., "Modern Probability Theory and its Applications," Wiley, 1960.
3. Longuet-Higgengs, M. S., "On the Statistical Distribution of the Heights of Sea Waves," Journal of Marine Research, Vol. XI, 1952.
4. Cartwright, D. E., and Longuet-Higgengs, "The Statistical Distribution of the Maxima of a Random Function," Proceedings of Royal Society of London, Series A, Vol. 237, 1956.
5. Crandahl, S. H. and Mark, W. D., "Random Vibration in Mehcanical Systems," Academic Press, New York, 1963.
6. Jasper, N. H., "Statistical Distribution Patterns of Ocean Waves and Wave Induced Ship Stresses and Motions with Engineering Applications," Transactions, Society of Naval Architects and Marine Engineers, Vol. 64, 1956.
7. Bledsoe, et al, "Seakeeping Trials on Three Dutch Destroyers," Transactions, Society of Naval Architects and Marine Engineers, Vol. 68, 1960.
8. Vassilopoulos, L. A., "A Compendium of Results from the Theory of Random Processes for Application to Seakeeping," M.I.T., Department of Naval Architecture and Marine Engineering, Report No. 65-10.
9. Abramobitz and Stegun, "Handbook of Mathematical Functions," Dover.
10. Parissis, G., "The Effect of Hull Shape Non-linearities on the Calculation of Heave and Pitch of a Ship," M.I.T., Department of Naval Architecture and Marine Engineering, Report No. 64-6.

11. Korvin-Kroukovsky, B. V., "Theory of Seakeeping", The Society of Naval Architects and Marine Engineers, 1961.

12. Williams, A. J. and Cartwright, D. E., "A Note on the Spectra of Wind Waves," Transactions, American Geophysical Union," Vol. 38, No. 6, December 1957.

APPENDIX A. Computer Program

The computer program, as described in Section 4, Part B, calculates the ratios $\tilde{H}^{(p)}/\tilde{H}_{RMS}$. The program is divided into two parts, MAIN Program and subroutine ORDER. The FORTRAN Listing of MAIN and the FAP Listing of ORDER appear in the following.

LIST OF COMPUTER PROGRAM VARIABLES AND CONSTANTS

Program Symbol	Text Symbol	Meaning
AP	$\tilde{H}^{(P)}/\tilde{H}_{R.M.S}$	Values of the $1/n=P$ highest apparent heights over the root mean square apparent height
DEV	$\tilde{H}_{RM.S.}$	Root mean square apparent height
DELTH	$\tilde{H}$	Calibration for digitizing rate Apparent height
HSUM	$\tilde{H}^{(P)}$	Values of the $1/n=P$ highest apparent heights
HVAR	σ^2	Variance of the process
IDENT		Identification of the process
K(N)		Values of digitized data. Departures from mean level of the process
KMAX(N)	$\tilde{A}_C$	Apparent amplitude of a crest
KMIN(N)	$\tilde{A}_T$	Apparent amplitude of a trough
KTMAX(N)		Order of a crest among the data points
MEAN		Mean level of the process
MT		Number of data points
NMAX		Number of crests
NMIN		Number of troughs
SCALE		Calibration for apparent heights
SCALT		Calibration for apparent periods
T	$\tilde{T}$	Apparent period

```
C       THIS PROGRAM CALCULATES THE RATIOS OF THE 1/N HIGHEST APPARENT
C       HIGHTS OVER THE RMS APPARENT HEIGT OF A RANDOM PROCESS
        DIMENSION K(10000),KMAX(1300),KTMAX(1300),KMIN(130 ),H(1300),
       1T(1300),NP(9),NX(9),Q(9),P(9),AP(9),HSUM(9)
        COMMON K,KMAX,KTMAX,KMIN,H,T,NP,NX,Q,P,AP,NT,M,NL,NN,NTA,NSTOP,
       1  NMAX,NMIN,NA,MAX,MTMAX,MIN,NMIN,KX,NA,NB,HVAR,BUG,DELT,AN1,
       2 DEV,ANMIN,HSUM,SCALE,DELT,MT,IDENT,MEAN,SCALT
  10    READ 100,IDENT,MT,SCALE,DELT,SCALT
 100    FORMAT(2I8,3F8.4)
        PRINT 120, IDENT
 120    FORMAT(I8//)
        DO  998    N=1,1300
        H(N)=0.
 998    CONTINUE
        DO 999J=1,9
        AP(J)=0.
 999    CONTINUE
        IF(IDENT)  38,38,26
  26    NT=24*MT
        READ 101,(K(N),N=1,NT)
 101    FORMAT(24I3)
C       NT=TOTAL NUMBER OF POINTS IN WAVE RECORD
        AMEAN=0.
        DO 50          N=1,NT
```

```
      AMEAN=AMEAN+AK
      AK=K(N)
   50 CONTINUE
      ANT=NT
      AMEAN=AMEAN/ANT
      MEAN=AMEAN
      PRINT 102 , MEAN
  102 FORMAT(6H MEAN=,I3//)
      DO 40      N=1,NT
      K(N)=K(N)-MEAN
   40 CONTINUE
      PRINT 301 , K
  301 FORMAT(30I4)
C     LOOKING FOR FIRST COMPLETE CREST
      IF(K(1))   1,2,5
    2 DO 3       N=2,NT
      M=N
      IF(K(N))   4,3,8
    3 CONTINUE
      GO TO 99
    1 NL=2
      GO TO 6
    4 NL=M+1
    6 DO 7       N=NL,NT
      M=N
      IF(K(N))   7,8,8
```

```
    7   CONTINUE
        GO TO 99
    5   DO 9        N=2,NT
        M=N
        IF(K(N))  4,4,9
    9   CONTINUE
        GO TO 99
C       K(M) IS THE FIRST POINT OF THE FIRST COMPLETE CREST
C       ELIMINATING RECORD AFTER LAST COMPLETE CREST
        NN=NT-M
        NTA=NT+1
        IF(K(NT))  11,12,15
   12   DO 13       N=2,NN
        J=NTA-N
        IF(K(J))  14,13,18
   13   CONTINUE
        GO TO 99
   11   NL=2
        GO TO 16
   14   NL=NTA-J+1
   16   DO 17       N=NL,NN
        J=NTA-N
        IF(K(J))  17,18,18
   17   CONTINUE
        GO TO 99
   15   DO 19       N=2,NN
```

```
      J=NTA-N
      IF(K(J)) 14,14,19
19    CONTINUE
      GO TO 99
18    NSTOP=J
      PRINT 303 , NSTOP
303   FORMAT(1H ,I4)
C     K(NSTOP) IS THE LAST POINT OF THE LAST COMPLETE CREST
C     NUMBER OF POINTS REMAINING IN RECORD=NSTOP-M
      NMAX=0
      NMIN=0
C     LOOKING FOR A CREST
32    NA=M+1
      MAX=K(M)
      MTMAX=M
      IF(NA-NSTOP)  24,24,99
24    DO 20      N=NA,NSTOP
      M=N
      IF(K(N))   21,21,22
22    IF(K(N)-MAX)   20,20,23
23    MAX=K(N)
      MTMAX=M
20    CONTINUE
21    NMAX=NMAX+1
      KMAX(NMAX)=MAX
      KTMAX(NMAX)=MTMAX
```

```
C       LOOKING FOR A TROUGH
        NA=M+1
        IF(NA-NSTOP)   27,25,25
   27   MIN=K(M)
        DO 28      N=NA,NSTOP
        M=N
        IF(K(N))   29,30,30
   29   IF(K(N)-MIN)   31,28,28
   31   MIN=K(N)
   28   CONTINUE
        GO TO 99
   30   NMIN=NMIN+1
        KMIN(NMIN)=MIN
        GO TO 32
C       ALL CRESTS AND TROUGHS LOCATED.  COMPUTE WAVE HEIGHTS AND PERIODS
   25   PRINT 103, NMAX, NMIN
  103   FORMAT(17H NO OF CRESTS IS ,I4,18H NO OF TROUGHS IS ,I4//)
        HVAR=0.0
        DO 33      N=1,NMIN
        BUG=KMAX(N)+KMAX(N+1)-2*KMIN(N)
        H(N)=0.5*BUG*SCALE
        HVAR=HVAR+H(N)**2
        BUG=KTMAX(N+1)-KTMAX(N)
        T(N)=DELT*BUG*SCALT
   33   CONTINUE
        AN1=NMIN-1
```

```
      HVAR=HVAR/AN1
      DEV=SQRTF(HVAR)
      PRINT 104,HVAR,DEV
  104 FORMAT(6H HVAR=,F10.3,4H FT2,8H   DEV=,F8.3,2HFT//)
C     ARRANGE WAVE HEIGHTS IN DECREASING ORDER
      CALL ORDER(H,T,NMIN)
      PRINT 105, H
  105 FORMAT(16H WAVE HEIGTS FTS/(1H ,20F6.1))
      PRINT 110 , T
  110 FORMAT(17H WAVE PERIODS SEC/(1H ,12F10.4))
C     H(1) IS NOW THE LARGEST WAVE
      HMAX=H(1)
      PRINT 106, HMAX
  106 FORMAT(21H THE LARGEST WAVE IS ,F6.1//)
C     COMPUTE AVERAGE OF P-TH HIGHEST WAVES-FROM 1/500 TO 1/1
      ANMIN=NMIN
      NP(1)=500
      NP(2)=100
      NP(3)=50
      NP(4)=20
      NP(5)=10
      NP(6)=5
      NP(7)=3
      NP(8)=2
      NP(9)=1
      NX(1)=0
```

```
      KX=2
C     SKIP ANY FRACTION CONTAINING LESS THAN  NP(L) WAVES
      DO 34     L=1,9
      IF(NMIN-NP(L))  34,35,35
 35   NX(KX)=NMIN/NP(L)
      Q(KX)=NX(KX)
      P(KX)=Q(KX)/ NMIN
      KX=KX+1
 34   CONTINUE
      PRINT 107
 107  FORMAT(89H AVERAGES OF THE 1/NP(L) HIGHEST WAVES OVER RMS WAVE HEI.
     1GHT ENDING BY THE RATIO AP(1)/RMS//)
      KX=KX-1
      HSUM=0.0
      DO 36      J=2,KX
      NA=NX(J-1)+1
      NB=NX(J)
      DO 37      N=NA,NB
      HSUM=HSUM+H(N)
 37   CONTINUE
C     AP IS THE AVERAGE OF THE P-TH HIGHEST WAVES-OVER RMS WAVE HEIGHT
      AP(J-1)=HSUM/(Q(J)*DEV)
 36   CONTINUE
      PRINT 109, AP
 109  FORMAT(5H  AP=,9F7.4)
      GO TO 10
```

```
      38   CALL EXIT
           CALL EXIT
           END


C          SUBROUTINE ORDER IN FAP
           COUNT   35
           ENTRY   ORDER
           REM     REORDERS X IN INCREASING ORDER FOR FORTRAN
           REM     AND DUPLICATES SHIFTS IN K
     ORDER SXA     XR,2
           SXA     XP+1,1
           CLA*    3,4                 N=NUMBER IN LIST
           ARS     18
           STA     A9
           CLA     1,4                 HIGH END OF X
           ADD     =1
           STA     A5
           STA     A2
           STA     A1
           STA     A1+1
           CLA     2,4                 HIGH END OF K
           ADD     =1
           STA     A1+2
           STA     A1+3
           STA     A1+4
```

```
        STA     A1+5
A9      AXT     **,3
A7      TNX     XR,1,1
        SXD     A10,1
A5      LDQ     **,2            X+N
A2      CLA     **,1            X+N
        TLQ     A1              X(1) LESS THAN X(2)
A3      TIX     A2,1,1          X(1) GREATER OR = X(2)
A10     TXI     A4,0,**         XR1 PARKED IN DECREMENT
A1      STQ     **,1            X+N
        STO     **,2            X+N
        CLA     **,2            K+N
        LDQ     **,1            K+N
        STQ     **,2            K+N
        STO     **,1            K+N
        TIX     A5,1,1
A4      LXD     A10,1
        TIX     A7,2,1
XR      AXT     **,2
        AXT     **,1
        TRA     4,4
        END
*       DATA
C       THE PROGRAM EXPECTS ONE CARD WITH THE VALUES OF IDENT,MT,SCALE,
C       DELT,SCALT WITH FORMATS AS IN STATEMENT 100.THEN MT CARDS WITH
C       THE DIGITIGED DATA WITH FORMAT 24I3
```